IEEE Access
Multidisciplinary | Rapid Review | Open Access Journal

Received May 24, 2021, accepted June 26, 2021, date of publication June 30, 2021, date of current version July 26, 2021.

Digital Object Identifier 10.1109/ACCESS.2021.3093696

High-Voltage Stations for Electric Vehicle Fast-Charging: Trends, Standards, Charging Modes and Comparison of Unity Power-Factor Rectifiers

IKER ARETXABALETA, IÑIGO MARTÍNEZ DE ALEGRÍA, JON ANDREU, IÑIGO KORTABARRIA, AND ENDIKA ROBLES

Faculty of Engineering, University of the Basque Country (UPV/EHU), 48013 Bilbao, Spain

Corresponding author: Iker Aretxabaleta (iker.aretxabaleta@ehu.eus)

This work was supported in part by the Government of the Basque Country through the Fund for Research Groups of the Basque University System under Grant IT978-16, in part by the Research Program ELKARTEK under Project ENSOL2-KK-2020/00077 and Project HARVESTGEN-KK-2020/00113, in part by the Ministerio de Ciencia e Innovación of Spain under Project PID2020-115126RB-I00, and in part by the FEDER Funds.

ABSTRACT Emission of greenhouse gases and scarcity of fossil fuels have put the focus of the scientific community, industry and society on the electric vehicle (EV). In order to reduce CO_2 emissions, cutting-edge policies and regulations are being imposed worldwide, where the use of EVs is being encouraged. In the best of scenarios reaching 245 million EVs by 2030 is expected. Extensive use of EV-s requires the installation of a wide grid of charging stations and it is very important to stablish the best charging power topology in terms of efficiency and impact in the grid. This paper presents a review of the most relevant issues in EV charging station power topologies. This review includes the impact of the battery technology, currently existing standards and proposals for power converters in the charging stations. In this review process, some disadvantages of current chargers have been identified, such as poor efficiency and power factor. To solve these limitations, five unidirectional three-phase rectifier topologies have been proposed for fast EV charging stations that enhance the current situation of chargers. Simulation results show that all the proposed topologies improve the power factor issue without penalizing efficiency. The topologies with the best overall performance are the Vienna 6-switch and the Vienna T-type rectifier. These two converters achieve high efficiency and power factor, and they allow a better distribution of losses among semiconductors, which significantly increase the life-cycle of the semiconductor devices and the reliability of the converter.

INDEX TERMS Electric vehicle standards batteries charging modes three-phase rectifier Vienna rectifier power factor.

I. INTRODUCTION

Protection of the environment has become one of the main concerns of social agents, policy makers and the scientific community due to factors such as greenhouse gas (GHG) emissions, scarcity of fossil fuels and volatility of their prices. The long-term European Commission strategic vision for a modern, competitive and climate-neutral economy indicates the tendency that GHG emissions should follow [1]. By 2050 the goal of not raising the planet temperature by more than 1.5 ^{o}C could be achieved. However, according to the projections of the International Energy Agency (IEA), GHG emissions are expected to double by 2050 from 2005 levels [2]. In this sense, United States Environmental Protection Agency (EPA) states in [3] that transportation is one of the sectors that contributes the most to GHG emissions, producing, nowadays, approximately 28 % of the total emissions.

According to United Nations reports, the world population will reach 9.7 billion inhabitants in 2050 (which represents an increase of practically 33 % compared to the 2015 population of 7.3 billion inhabitants [4]) and the expected number of

The associate editor coordinating the review of this manuscript and approving it for publication was Wei Xu.

road vehicles will be around 2 billion in 2050 [5]. In this context, the electrification of the transport sector in general, and that of road vehicles in particular, becomes essential to overcome the environmental problems mentioned above. This challenge demands improvements in all the power chain of the electric vehicle (batteries, power converters, semiconductors, charging stations...), providing innovative solutions that facilitate end-customer access to the electric vehicle (EV) [6], [7]. With this objective, several initiatives and campaigns are being promoted worldwide: Electric Vehicles Initiative (EVI) [8], EV30@30 campaign [9], EV100 [10], Global EV Pilot City program [2], Drive to Zero campaign [2], GEF-7 global program [11], etc.

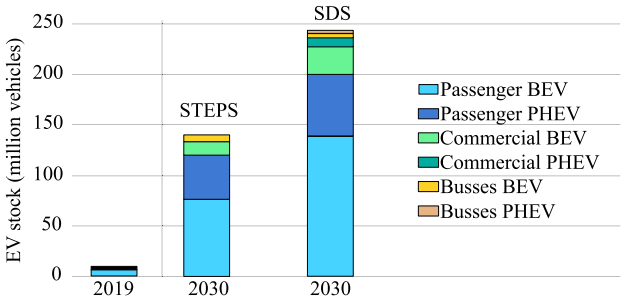

FIGURE 1. Global electric vehicle stock by scenario 2019-2030 (IEA) [2].

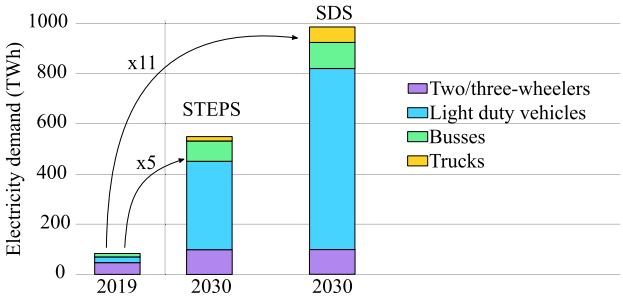

FIGURE 2. Electric vehicle charging energy demand (IEA) [2].

Regarding EV sales, the IEA [2] estimates that the global stock of EVs can reach 140 million by 2030 with stated policy scenarios (STEPS), and if ambitious sustainable development scenarios (SDS) are implemented, it would reach 245 million units (see Fig. 1). In this sense, the IEA forecasts a surge in the global electricity demand of EVs, in both stated policies scenarios and sustainable development scenarios (Fig. 1-STEPS and Fig. 1-SDS) [2]. As it can be seen in Fig. 2, an increase around 550 TWh is expected from 2019 to 2030 according to STEPS. Conversely, in the SDS scenario reaching 1000 TWh is expected, which is equivalent to an 11 fold increase compared to 2019. While EVs today represent a small fraction of total electricity consumption (globally less than 0.5 %), this will change in the future. According [2], in 2030 EVs could represent between 1-4 % of global electricity consumption in the STEPS scenario and between 2-6 % in the SDS [2].

In such a context, the EV takes on a lot of relevance for the grid. The grid will have to be dimensioned so that these demands will not become a source of problems for the electrical supply system. Many aspects need to be considered: change of peak and valley hours in the demand curve, re-evaluation of rating of the power grid and others. During the past few years there has been a focus on increasing grid power quality. Today the greatest part of the harmonic distortion in the electric grid is caused by the input stage of power electronic converters. International standards, such as IEEE 519 and EN 61000, set the limits to power quality-related parameters (harmonic currents and voltages). Moreover, the power factor (PF) is one of the key performance parameters for a grid without distortion, where power factor $(PF) \simeq 1$ is necessary for that purpose [13].

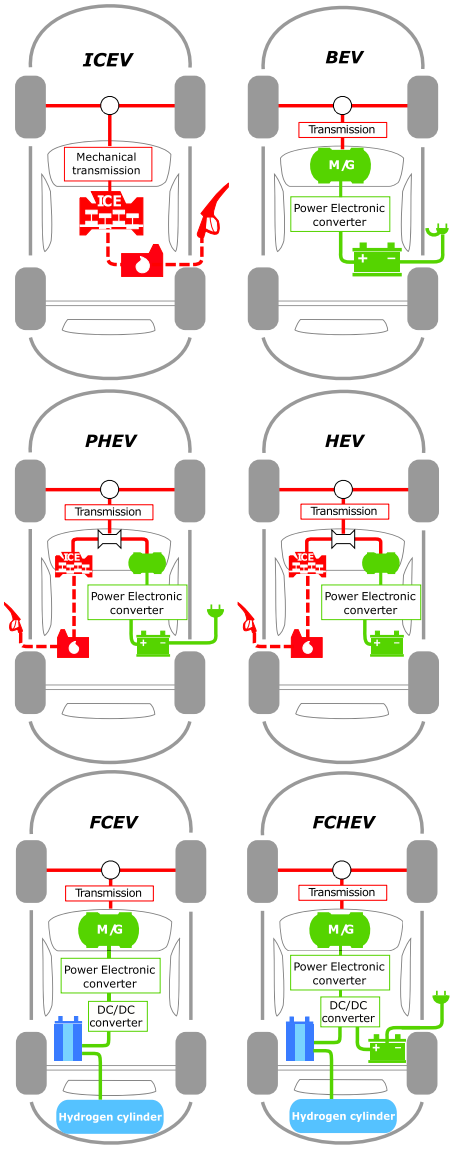

FIGURE 3. Most relevant vehicle architectures according to their propulsion system (adapted from [12]).

Regarding the electrification of the vehicles, there are several alternatives (see Fig. 3) to internal combustion engines (ICE) [14]–[20]: battery electric vehicles (BEV), plug-in

TABLE 1. Examples of commercial electric vehicle models and their characteristics (BEV and PHEV).

Manufacturer	Model	Power (kW)	Type	Battery (kWh)	Battery Voltage (V)	Autonomy (km) [a]
BMW	i3	137	BEV	42.2 (Li-Ion)	360	359
	I3s	137	BEV	42.2 (Li-Ion)	360	344
	iX3	213	BEV	74 (Li-Ion)	– [b]	360
Mercedes-Benz	EQC	304	BEV	80 (Li-Ion)	405	409
	EQV	152	BEV	90 (Li-Ion)	– [b]	418
Nissan	Leaf e+	162	BEV	62 (Li-Ion)	384	385
	Ariya	225	BEV	87 (Li-Ion)	320	500
Porsche	Taycan 4S	395	BEV	93,4 (Li-Ion)	800	464
Renault	Zoe	101	BEV	52 (Li-Ion)	346	390
Tesla	Model S	593	BEV	100 (Li-Ion)	350	610
	Model 3	635	BEV	75 (Li-Ion)	300	530
	Model X	593	BEV	100 (Li-Ion)	350	487
	Model Y	465	BEV	100 (Li-Ion)	350	480
Toyota	Rav4 [c]	228	PHEV	18 (Li-Ion)	386	65
	Prius [c]	101	PHEV	8.8 (Li-Ion)	– [b]	40
Volkswagen	e-up	62	BEV	32.3 (Li-Ion)	307	258
	e-Golf	101	BEV	35.8 (Li-Ion)	323	198
	ID.3	152	BEV	82 (Li-Ion)	323	549
	ID.4	152	BEV	77 (Li-Ion)	– [b]	520
	Golf GTE	152	PHEV	13 (Li-Ion)	345	40
	Passat GTE	163	PHEV	13 (Li-Ion)	345	55

[a] World harmonized Light-duty vehicles Test Procedure (WLTP): harmonized standard for determining pollution, CO_2 emissions and fuel consumption of traditional and hybrid cars, as well as the range of fully electric vehicles.
[b] Data not provided by manufacturers.
[c] Models ready to go on the market in 2021.

hybrid electric vehicle (PHEV), hybrid electric vehicles (HEV), fuel cell electric vehicles (FCEV), and fuel cell hybrid electric vehicles (FCHEV). Nowadays, there is a trend among manufacturers towards BEV and PHEV and it seems that it will be maintained in the near future [14], [21]. Table 1 shows some examples of commercialized electric vehicles (BEV) and plug-in hybrids (PHEV).

The majority of light EVs are equipped with battery packs with nominal voltage range between 300 V and 420 V, while for heavy EVs this voltage can reach up to 800 V [22]. However, according to some studies [23]–[27], a change in trend is expected in the battery voltage of light EVs, and an increase in the DC bus to 800 V systems[1] is expected. With this change, a substantial reduction in the conductive wire weight could be achieved, since half the current will be handled for the same power [23]. Increasing the voltage of the battery pack would also reduce quadratic conduction losses ($P = I^2 R$). Therefore, with this change in the battery voltage, the efficiency of the EV will be improved. Battery voltage has a great impact in the selection of the charging station power converter topology. Section II presents the most extended types of batteries and their expected evolution for 2030. In section III, the standards applicable to each of the stages of the recharging system are reviewed. In addition, the charging modes that support current EVs and the types of existing charging stations are reviewed, and also a study of DC fast-charge stations from different manufacturers is carried out. In Section IV, a classification of valid power converter topologies for the fast-charging application is shown from a general perspective. Finally, in Section V, a comparison is made between the most suitable topologies selected with the criteria of high efficiency, unity power factor, and high power rating for fast-charging.

[1] An example is the Porsche Taycan, the first production vehicle with a system voltage of 800 V instead of the usual 400 V for electric vehicles.

II. BATTERIES: CURRENT STATUS AND FUTURE PROSPECTS

Batteries play a crucial role in making EVs competitive against ICEs [28], [29]. The batteries, apart from supplying energy to EVs, can also act as energy storage systems (ESS) for the grid. Charging the batteries in the hours of less energy demand (off-peak hours) and then providing that energy in the periods with higher demand [30]–[32] enables to make the energy demand curve flatter, with the benefits that this entails [33]–[37]. According to the International Renewable Energy Agency (IRENA), using ESSs would reduce energy installation costs between 50 % and 66 % (see Fig. 4) [38].

As far as battery technologies are concerned, there are no one-size-fits-all solutions in the ESS, and the decision to opt for one storage technology over another depends on several parameters, such as power density, lifetime, efficiency and operation temperature [39], [40]. In this context, some of the best known materials for battery systems are lead-acid [41]–[43], nickel-cadmium [44], [45] and lithium-ion [46]–[48]. Lead-acid batteries are one of the most mature and inexpensive battery technologies [38], [41], [49] but they are not as suitable as lithium-ion for EV application, since

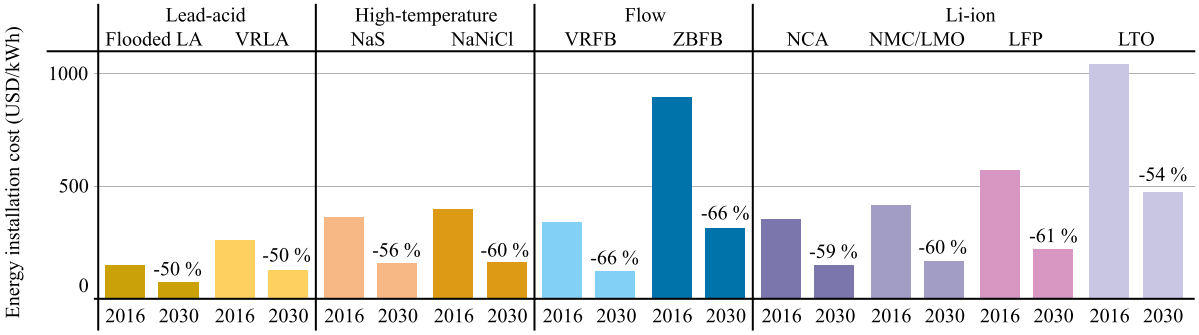

Note: LA=lead-acid; VRLA=valve-regulated lead-acid; NaS=sodium sulphur; NaNiCl=sodium nickel chloride; VRFB=vanadium redox flow battery ZBFB=zinc bromine flow battery; NCA=nickel cobalt aluminium; NMC/LMO=nickel manganese cobalt oxide/lithium manganese oxide; LFP=lithium iron phosphate; LTO=lithium titanate.

FIGURE 4. Energy cost reduction potential installing ESS classified by battery types [38].

TABLE 2. Evolution of battery technology by 2030 [40].

Features		Lead-based		Alkaline		Lithium-Ion	
		Pb 2020	Pb 2030	Nix 2020	Nix 2030	Lithium Ion 2020	Lithium-Ion 2030
Electro-chemical material	Cathode	PbO2	PbO2	B-NiOOH	B-NiOOH	NCM 111 (G.2a) NCM 523-622 (G.2b) LFP LMO LCO NCA	NCM 622-811 (Gen 3a) NCM811 HE-NCM HVS (Gen 3b) Solid State
	Anode	Pb, Pb+C	Pb, Pb+C	Cd, MH	Cd	LTO, C (G2a2b)	C+Si(5-10%) (Gen 3a) Si/C (Gen 3b)
Energy density [Wh/kg]	Cell System	$24-48$ $23-45$	$30-60$ $35-55$	$28-50$ $24-43$	$30-55$ $38-50$	$60-250$ $20-140$	$300-450$ $80-400$
Energy density [Wh/l]	Cell System	$60-105$ $36-100$	$80-150$ $50-110$	$55-80$ $47-70$	$60-90$ $50-75$	$140-580$ $20-250$	$650-1100$ $100-1000$
Power density [W/kg]	Cell System	$34-448$ $41-400$	$80-505$ $65-450$	$80-225$ $68-180$	$100-240$ $80-210$	$210-1800$ $170-520$	$450-1100$ $250-700$
Power density [W/l]	Cell System	$91-880$ $76-840$	$120-920$ $72-900$	$112-400$ $95-350$	$120-460$ $100-380$	$470-2200$ $180-650$	$800-2500$ $600-1200$
Lifetime	Cycles Years	$200-2500$ $10-25$	$1000-4800$ $10-25$	3000 20	4000 20	>3500 10	>10.000 $15-25$
Op. Temp. (^oC)		$-25\ to\ +50$	$-25\ to\ +50$	$-50\ to\ +60$	$-50\ to\ +60$	$0\ to\ +45$ charge $-20\ to\ +60$ disch. $-30\ to\ +55$ LTO	$-30\ to\ +60$
Efficiency (%)		$67-85$	>90	$70-85$	>85	>90	95
Recycling (%)		90	90	79	$80-85$	50	$80-85$

their energy density is low [42]. Even so, they are still widely used for the stabilization of the grid [43]. Nickel-cadmium batteries serve special markets where energy must be stored in extreme weather conditions, as they work well where temperatures are very low (down to $-40\,^oC$) [44]. The biggest drawback to using them in the application of the EV is its high price and low power density [44]. In this context, lithium-ion batteries have entered the industrial market (see Table 1), drawing on the extensive experience gained in developing batteries for electric and hybrid vehicles. The choice of lithium-ion for EVs is justified by high energy density, low-charge operation capability [47], [48] and long lifetime which could reach the full EV operating life [40]). This technology is versatile, highly scalable and can be adapted to almost any power requirement [40], [46].

According with the Association of European Automotive and Industrial Battery Manufacturers (EUROBAT), Table 2 shows how lead-acid, nickel-cadmium and lithium-ion batteries will be improved by 2030 [40]. These three types of batteries tend to improve their efficiencies (here lithium-ion batteries achieve 95 % efficiency, 5 % and 10 % higher than lead-acid and nickel-cadmium respectively), power densities (lithium-ion batteries are expected to reach 1100 Wh/l, more than 7 times greater than its most direct rival, lead-acid), recycling capabilities (lithium-ion is expected to improve the most, until almost reaching lead-acid batteries recycling capacity of 90 %) and lifetime (here lithium-ion reaches >10.000 life cycles, twice that of its competitors) [40]. EV manufacturers are currently selecting lithium-ion batteries and it seems that in the near future this trend will not change, since none of the other battery materials reach the levels of power density required in EVs. In addition, according to the international organization Bloomberg-NEF [50], [51], the price trend of batteries is downward

TABLE 3. Overview of the most important standards for EV charging stations [52].

	Fig. 6 stage	International	America	Japan	China	Taiwan
General requirements	1	IEC 61851-1	NEC 625 SAE J1772 UL 2231-1 UL 2231-2	JEVS G109	GB/T 18487.1	CNS 15511-2 CNS 15511-3
Communications	1	IEC 61851-24	SAE J2293-1 SAE J2293-2 SAE J2847-2	CHAdeMO	GB/T 27930	-
EV connection	4	IEC 61851-21	-	-	GB/T 18487.2	CNS 15511-3
Plugs & cable assembly	4	IEC 62196-1 IEC 62196-2 IEC 62196-3	SAE J1772 UL 2251	JEVS C601 JEVS G105	GB/T 20234.1 GB/T 20234.2 GB/T 20234.3	CNS 15511-2 CNS 15511-3
AC charger	5	IEC 61851-22	UL Sub. 2594	-	GB/T 18487.3	CNS 15511-3
DC charger	6	IEC 61851-23	UL 2202	JEVS G101 JEVS G103 CHAdeMO	GB/T 18487.3	CNS 15511-3

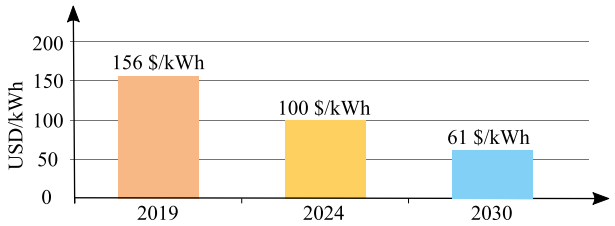

FIGURE 5. Battery pack average price projection [50].

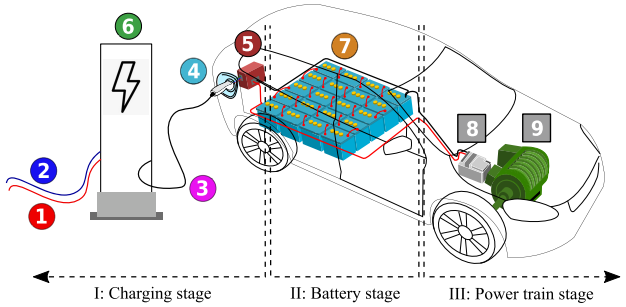

FIGURE 6. Electric vehicle charging station standardized stages (blocks 1 to 6), battery stage and power train stages.

(see Fig. 5), which will make lithium-ion technology much more competitive.

III. ELECTRIC VEHICLE: STANDARDS, CHARGING MODES AND CHARGING STATIONS

Electric vehicle charging points [1], [2], [8], [9] are spreading around the world due to the growing demand of EVs. This has led to the regulation of charging stations. In this context, there are several standards defined by organizations for EV charging established worldwide [52]–[55]: IEC, SAE, IEEE, GB/T, CHAdeMO, among others. Figure 6 shows the electric stages of an EV: (I) the charging stage, (II) the battery stage (where there is a 7 battery system, which is charged through the stage (I)) and finally, (III) the power train (composed by the power converter 8 and the electric motor 9 which is responsible for transmitting the power to the wheels). Regarding (I) the charging stage, there are standards related to 1 the grid power-connection, 1 the grid central management system communications, 4 the EV charging cable power and communication capability, 5 the vehicle connectors, 5 the battery management system (it can be an on-board charger, if not, 6 can act as off-board charger).

Table 3 summarizes the standards(Fig. 6 - 1 to 6) classified by regions. The EV charging modes are included in the IEC 62196 (international standard for the set of electrical connectors and charging modes), IEC 61851 (international standard for conductive electric vehicle systems) and SAE J1772 (general physical, electrical, communication protocol and performance requirements) standards, used in Europe and in USA, respectively. These regulations are being updated as technology matures, adapting to increasing power ratings for lower charging times.[2]

Regarding the EV charging modes (see Table 4), some of best known battery charging modes are described in the IEC 61851, IEC 62196 and SAE J1772 standards. The charger power ranges from 4 kW (IEC 61851-1:2020, mode 1) to 600 kW (IEC 61851-23:2014, mode 4), which shows that these regulations contemplate a wide range of chargers. Special attention should be paid to the fastest chargers (120-600 kW) since they would decrease the anxiety of EV owners caused by the lack of large autonomy-range and the non-possibility of fast-charging [24], [57]–[63]. In this sense, many manufacturers are working in EV fast-charging system development. Some of them are shown in Table 5. According to the data provided by these manufacturers the power converters have an efficiency of 94-95 %.

Another important aspect that characterizes the charging station is the power factor (1. A suitable electric vehicle charger is one that demands unity power factor, $PF = 1$.

[2]Phoenix Contact is already manufacturing connectors that comply with the IEC 62196-3-1 standard. These connectors reach 1000 V and 500 A, thus achieving powers of 500 kW, high powers that would accelerate the charging time of the EVs [56].

TABLE 4. Charging modes for the most important standards applied in EV charging systems.

Standards	Charging Mode	Max. Voltage (V)	Max. Current (A)	Power (kW)
IEC 62196-2:2016	1	250 V_{AC}	32	8
	2	250 V_{AC}	70	17,5
	2[a]	480 V_{AC}	63	30,24
	3	250 V_{AC}	70	17,5
	3[a]	480 V_{AC}	63	30,24
IEC 62196-3:2014	4 (AA)[b]	600 V_{DC}	200	120
	4 (BB)[b]	750 V_{DC}	250	187,5
	4 (EE)[b]	600 V_{DC}	200	120
	4 (FF)[b]	1000 V_{DC}	200	200
	4[c]	1000 V_{DC}	500	500
IEC 61851-1:2020	1	250 V_{AC}	16	4
	1	480 V_{AC}[a]	16	7,68
	2	250 V_{AC}	32	8
	2	480 V_{AC}[a]	32	15,36
	3[d]	250 V_{AC}	32	8
	3[d]	480 V_{AC}[a]	32	15,36
IEC 61851-23:2014	4	1500 V_{DC}	300[e]	450
SAE J1772	1	120 V_{AC}	16	1,92
	2	240 V_{AC}	<80	19,2
	3	240 V_{AC}	>80	19,2
	1	450 V_{DC}	80	36
	2	450 V_{DC}	200	90
	3	600 V_{DC}	400	240

[a] Three-phase grid.
[b] Used with charging points according to: Appendix AA, BB, CC of the IEC 61851-23:2014 standard.
[c] Phoenix Contact - Charging technology for electro-mobility (IEC 62196-3-1).
[d] Mode 3: connecting an EV to an AC power supply system permanently connected to an AC power grid, with a control pilot function comprising from the AC power supply system until the EV.
[e] Data provided in Table D.1 of IEC 61851-23:2014.

TABLE 5. Characteristics of some fast chargers according to the manufacturers.

Manufacturer	Model	Power (kW)	Efficiency (%)	PF	Max. Voltage (V_{DC})	Max. Current (A_{DC})
ABB	Terra 54 HV	50	94	0,96	920	125
Circontrol	Raption 50	50	95	0,98	500	125
Ingeteam	Rapid 50	50	94	0,98	500	125
Enel X	JuicePump 50	50	95	0,97	500	120
Setec Power	Setec Power	150	- [a)]	0,99	400	300
Efacec	HV350	160	95	- [a)]	920	1750
EVBox	Ultroniq V2	350	95	0,98	950	368

[a)] Data not provided by the manufacturer.

The distortion factor, (*DistF*), measures the effect of the total harmonic distortion (*THD*), and the displacement factor, (*DispF*), also known as $cos(\Phi)$, measures the effect of the phase displacement of the current first harmonic and the grid voltage. Figure 7 shows the different parameters affecting power factor. Assuming that $cos(\Phi)$ is equal to 1 in the converters in Table 5, from (1), the *PF* values provided by the manufacturers, between 0,96 and 0,99, would mean the THD_i is between 29 % and 14 %.

$$PF = \frac{P}{S} \Rightarrow PF = DistF \cdot DispF = \frac{1}{\sqrt{1 + THD_i^2}} \cdot cos(\Phi) \tag{1}$$

There is a need to improve harmonic distortion in the charging stations (THD_i). In this sense, a niche for improvement is the power converter of the battery chargers, where several topologies can provide power factor close to unity ($PF \simeq 1$). Section IV analyses alternatives of power converter topologies that can achieve these targets.

IV. UNIDIRECTIONAL THREE-PHASE RECTIFIERS FOR FAST EV CHARGING STATIONS

In the actual stage of development of technology users who normally require fast-charging do not act as power suppliers to the grid, and therefore the charger does not have to be bidirectional. In the short and medium term there is no ESS capability in the grid. Thus, fast-charging stations demand unidirectional rectifiers for users who need a quick emergency charge, those who do not have electric chargers at their homes,[3] and customers who are on long routes [65]–[67]. In this context, the converters (see Fig. 8) that meet the requirements of the energy demand of this type of customer can be divided in three main groups [68], [69]: *(1)* passive, *(2)* hybrid and *(3)* active rectifiers:

1) Passive rectifiers: these are low complexity rectifiers that are divided into two groups: single diode bridges and multi-pulse rectifiers. These type of topologies

[3] 37 % of U.S. house owners do not have a garage for EV charging [64].

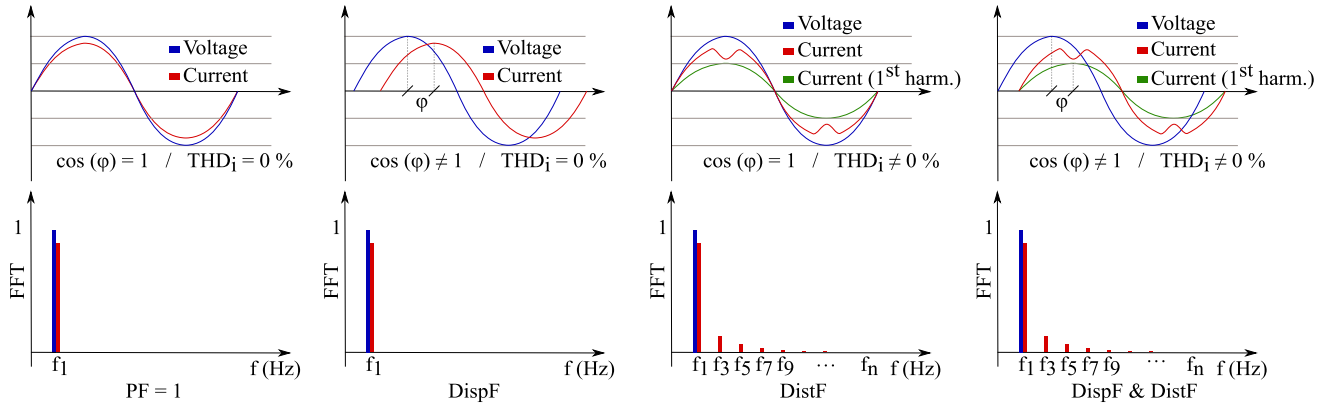

FIGURE 7. Distortions affecting the power factor: displacement factor (DispF) and distortion factor (DistF).

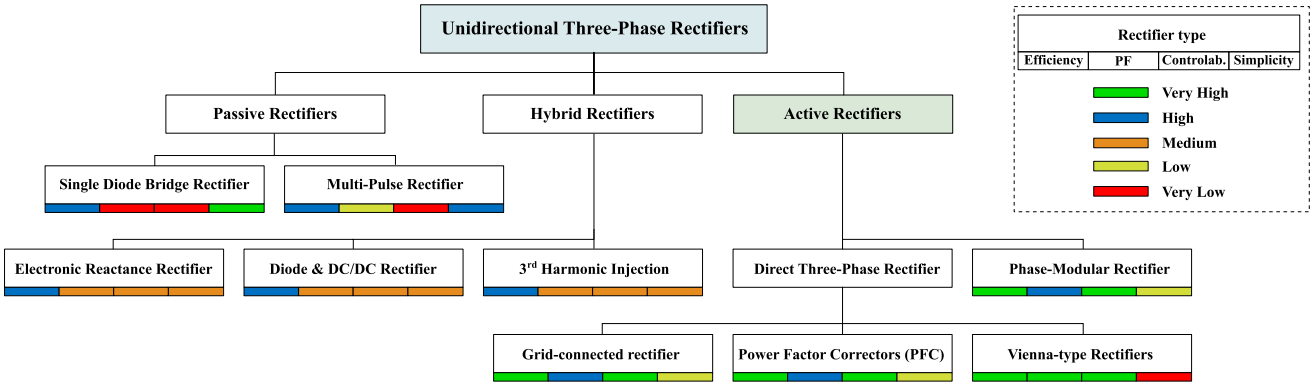

FIGURE 8. Classification of unidirectional three-phase rectifiers (adapted from [68], [69]).

allow easy implementation, but at the same time lack of controllability results in low quality input current and output voltages [68], [70], [71], which makes ageing of batteries worse [72]–[74].

2) Many of the unidirectional three-phase rectifiers that appear in the literature are located in the subset of hybrids rectifiers. They are divided into three groups: those based on reactance, those obtained by combining diodes and DC/DC converters and, finally, the topologies that allow injection of the third harmonic [68]. In general, the hybrid converters are made up of passive (capacitors and inductors) and active semiconductor devices, the latter being found in reduced quantities, increasing the degree of controllability compared to passive rectifiers. However, the quality of the output voltages given by the hybrid topologies is still not suitable for the EV charging application [68].
3) Active rectifiers are known for their high degree of controllability, synthesizing better input currents ($THD_i < 5\%$) and output voltages, and potentially they could achieve excellent efficiencies (up to 99%) [75]–[81]. These converters use higher amounts of active components compared to passive and hybrid rectifiers. Active rectifiers can be divided in two subgroups: direct and phase-modular systems. These topologies are used extensively in industry; however their use is rarely seen implemented for the EV charging application. This is due to the fact that currently (as Table 1 shows) most EVs use battery systems around 300-400 V. However, there is a change in trend towards 800 V battery systems [23]–[27]. In this context, this work focuses on boost-type unidirectional three-phase rectifier topologies, adapted to the trend towards 800 V battery systems [23]–[27]. These topologies are the most suitable for EV charging stations and they are selected for comparison in this work.

The scientific literature proposes several active three-phase rectifiers, which can be classified into (Fig. 8): Grid-connected rectifiers [82]–[96], Power Factor Corrector (PFC) [97]–[107] and Vienna rectifiers [108]–[118]. There is a large number of proposed converters, however, in order to reduce the number of studied converters, a parallel analysis of those topologies used by manufacturers has been made. Table 6 shows that most manufacturers use the following topologies: NPC, Vienna 6-switch rectifier, Vienna T-type and the three-phase two-level converter ($3\theta - 2L$).

As a result of the previous review the most suitable topologies for fast charging of high voltage batteries have been identified (see Fig. 9):

TABLE 6. EV fast-charging topologies by manufacturer.

	Vienna		Conventional rectifier	
Manufacturer	Type	Reference	Type	Reference
Fuji Electric	NPC	4MBI600VC-120-50	$3\theta - 2L$	7MBR75XWE120-50
	T-type	4MBI220VG-170R2-50	$3\theta - 2L$	6MBI100XBA120-50
	T-type	12MBI100VN-120-50	$3\theta - 2L$	6MBI550V-120-50
Infineon	6-switch	FS3L30R07W2H3FB11	$3\theta - 2L$	FS820R08A6P2B
	6-switch	F3L11MR12W2M1B65	$3\theta - 2L$	FS45MR12W1M1B11
	T-type	F3L400R12PT4B26	$3\theta - 2L$	DF80R07W1H5FPB11
Microsemi	NPC	APTMC60TLM14CAG	$3\theta - 2L$	MSCMC120AM02CT6LIAG
	NPC	APTMC60TLM55CT3AG	$3\theta - 2L$	APTMC120TAM12CTPAG
	T-type	APTMC120HRM40CT3AG		
Mitsubishi [a)]	AC-switch & Bridge	CM450C1Y-24T & CM300DY-34T	$3\theta - 2L$	CT1000CJ1B060
			$3\theta - 2L$	MSCMC120AM02CT6LIAG
Semikron	NPC	SKiM201MLI12E4	$3\theta - 2L$	SK50MH65TE1
	T-type	SKiM601TMLI12E4B	$3\theta - 2L$	SKiM459GD12F4V4
ST	T-type	STDES-VIENNARECT	$3\theta - 2L$	A2P75S12M3
			$3\theta - 2L$	A2C50S65M2
Vicontech	NPC	30PT07NAA300S501LF64F58Y	$3\theta - 2L$	80M3126PA200M7K820F70
	NPC	30FT07NIA320RVLE06F68	$3\theta - 2L$	30F2126PA150M7L280F79
	6-switch	10FZ071SA100SM02L526L18		
	T-type	70W612M3A1K8SC02L300FP70		
Vishay	-		$3\theta - 2L$	VS-ETY020P120F
Wolfspeed (Cree)	-		$1\theta - 2L$	CAB450M12XM3

Note: $3\theta - 2L$: three-phase two-level rectifier; $1\theta - 2L$: single-phase two-level rectifier.
[a)] Mitsubishi offers the possibility of joining two modules (AC-Switch and Bridge) to constitute a Vienna rectifier.

(a) **Conventional three-phase two-level rectifier** ($3\theta - 2L$) [119] is characterized by its simplicity and controllability (Fig. 9(a)). This topology is well positioned in the market. For this reason, it has been used as benchmark in this work. The semiconductor devices must block the voltage of the entire DC bus and the switching takes place between the two devices in each phase (one leg). Modulation and proper control techniques allow the voltage and current to be maintained in phase [83], [84]. However, two-level converters cannot synthesize the same waveforms quality as three-level topologies [120], [121].

(b) **Neutral Point Clamped converter (NPC)** [122] is a topology that can provide three voltage levels and is made up of twelve switches and six diodes (Fig. 9(b)). The devices must block half of the voltage of the entire DC bus [117]. This allows lower voltage rating semiconductors with lower conduction voltage drop. This topology also applies double effective frequency in the output, reducing the size of the output capacitors. High levels of efficiency (around 97 %) have been achieved with these converters [123]–[130]. These topologies have some drawbacks such as fluctuations on the output DC bus and mismatches in the distribution of losses between power devices [131], [132]. However, using suitable modulation techniques or additional control circuits, this problems can be minimized [133].

(c) **Vienna 6-switch rectifier** [68] is an adaptation of the original NPC topology in which non-current switches are turned-off during the rectifying operation. This topology is a three voltage level rectifier, it has six switches and twelve diodes (Fig. 9(c)) and can achieve very high efficiency (98%) [75], [76]. The semiconductor devices must block half of the voltage of the DC bus and high frequency switching takes place between one diode and the switch [117]. This topology greatly facilitates the process of precharging their output capacitors due to the path of the diodes [68]. However, one of the main drawbacks of this topology is the high number of devices.

(d) **The Vienna 3-switch rectifier** [134] (Fig. 9(d)), like the previous topology, is also classified among three-level voltage rectifiers. It is built by three switches and eighteen diodes. It reduces the number of controlled switches at the cost of increasing the number of simultaneously on devices to three units. The devices must block half the voltage of the entire DC bus and it can achieve a high efficiency (97-98 %) [77], [78]. The number of semiconductors can be considered its biggest disadvantage compared to other rectifiers. Among the analysed topologies, this is the one with the least number of active switches.

(e) **The Vienna T-type rectifier** [135], together with the Vienna 6-switch rectifier, is the most extended Vienna-type topology in the scientific literature. This topology is also a three voltage level rectifier. It is built by six diodes, making a three-phase diode rectifier and six switches forming three bidirectional switches (Fig. 9(e)). The devices must block all the DC bus voltage and the switching occurs between the diode and two series connected switches, one on diode-mode and the other in MOSFET-mode [117]. This topology can reach an efficiency

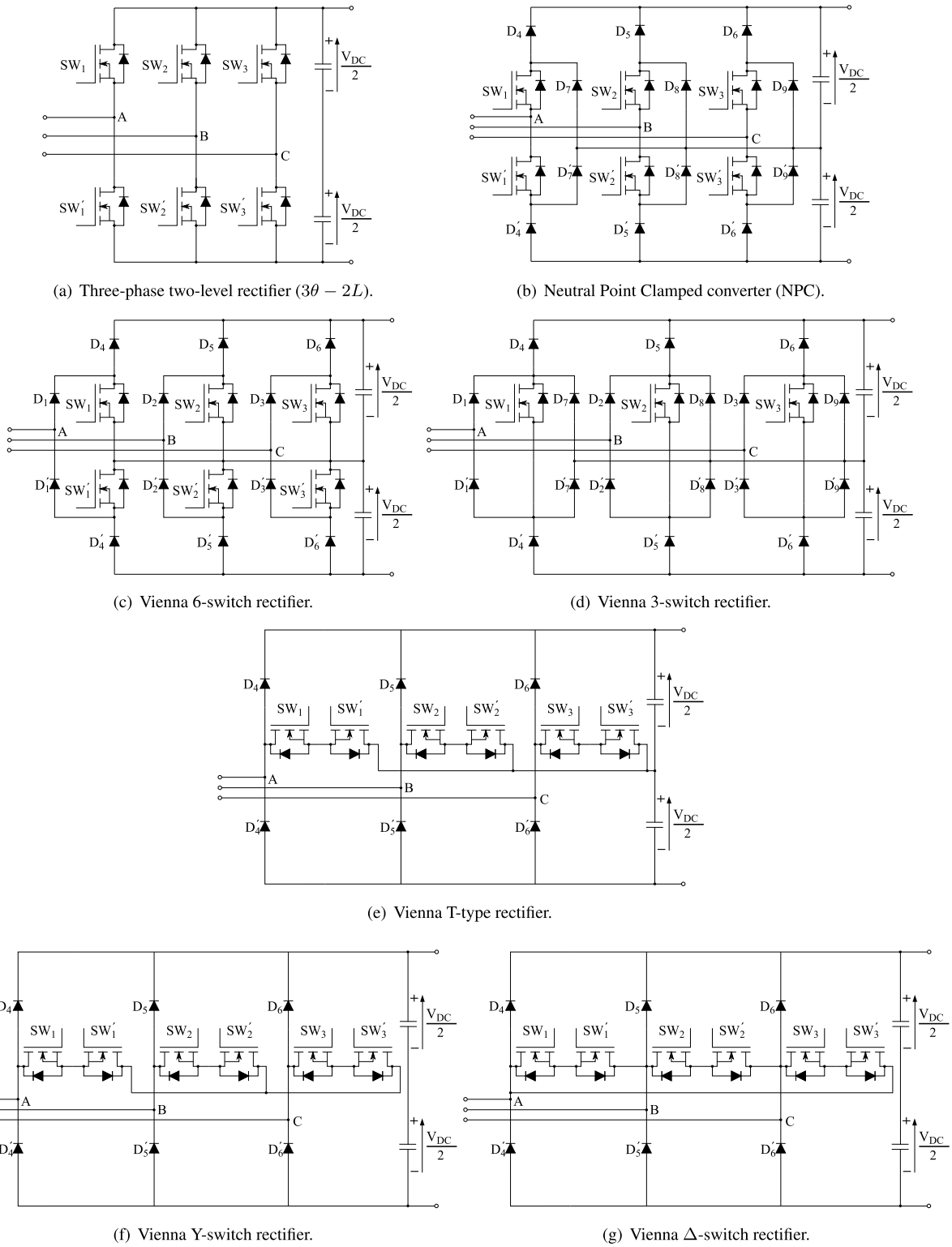

(a) Three-phase two-level rectifier ($3\theta - 2L$).

(b) Neutral Point Clamped converter (NPC).

(c) Vienna 6-switch rectifier.

(d) Vienna 3-switch rectifier.

(e) Vienna T-type rectifier.

(f) Vienna Y-switch rectifier.

(g) Vienna Δ-switch rectifier.

FIGURE 9. Rectifier topologies for EV fast-charging application.

of 94-98 % [79]–[81], however higher values (99 %) can be achieved using advanced modulations like interleaving technique [79]. The drawback of this topology is that in the fast commutation-cell three devices have to switch at the same time: a diode, and two MOSFETs. Furthermore, the MOSFETs carry current in both half cycles, therefore the losses are highly concentrated in these devices.

TABLE 7. Simulation setup parameters.

Simulation parameters			
Total system power	P	$50\ kW$	
Input line-to-line voltage 1	$V_{L-L_{rms}}$	$400\ V$	
Input coils 1	$L_{IN1}, L_{IN2}, L_{IN3}$	$500\ \mu H$	
Output voltage	V_{BUS}	$800\ V$	
Output capacitors 4	C_1, C_2	$3\ mF$	
Resistive load 5	R_{Load}	$12,8\ \Omega$	
Switching frequency	f_{SW}	$100\ kHz$	
Simulation step-size	t_{step}	$8,33\ ns$	
Semiconductor simulation model parameters			
MOSFET			
Reference	*Ref*	$C2M0025120D$	
Drain-Source voltage	V_{DS}	$1200\ V$	
Continuous Drain current	I_D	$60\ A@T_c = 100\ ^oC$	
Drain-Source on-state resistance	R_{DSon}	$43\ m\Omega@T_j = 150\ ^oC$	
Diode forward voltage	V_{SD}	$3,3\ V$	
Continuous diode forward current	I_S	$90\ A@T_c = 25\ ^oC$	
Reverse recovery current	I_{rrm}	$13,5\ A$	
Power dissipation	P_D	$463\ W@T_c = 25\ ^oC$	
Diodes			
Reference	*Ref*	$LSIC2SD120E40CC$	$SKKD8112$
Anode-Cathode voltage	V_{AK}	$1200\ V@T_j = 25\ ^oC$	$1200\ V@T_c = 87\ ^oC$
Continuous Forward current	I_F	$40\ A@T_c = 150\ ^oC$	$175\ A@T_c = 35\ ^oC$
Forward voltage	V_{Fmax}	$2,2\ V@T_j = 175\ ^oC$	$1,55\ V@T_j = 25\ ^oC$
Forward on-state resistance	R_F[a]	$32,5\ m\Omega$	$1,875\ m\Omega$
Power dissipation	P_D	$216\ W@T_c = 110\ ^oC$	$450\ W$

[a] Data extrapolated from the graphics of the datasheets.

(f)-(g) **The Y-switch** (Fig. 9(f)) and Δ-switch rectifiers (Fig. 9(g)) are alternatives of the T-type topology with variations of the composition of the T-type structures between phases. Since it is a two-level rectifier (the output bus is not split in two and connected to the midpoint), it is not possible to obtain the benefits of three-level rectifiers [120], [121]. For this reason, these two topologies are not considered as suitable for the EV charging application.

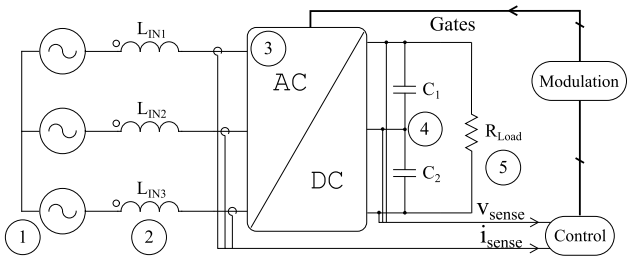

FIGURE 10. Simulation setup scheme for EV charging application.

V. COMPARISON OF SELECTED THREE-PHASE BOOST-TYPE RECTIFIERS FOR FAST EV CHARGING STATIONS

This section compares the topologies of interest for fast-charging of the EVs reviewed in the previous section through simulations performed with the PSIM simulation tool. For that purpose, a Forward Oriented Control (FOC) and Pulse Width Modulation (PWM) have been used. When analysing the results, several figures of merit have been taken into account, such as the number of devices and blocking voltage, efficiency, quality of input currents ($PF \simeq 1$, $THD_i < 5\%$, and $cos(\Phi) = 1$), quality of output voltage (low voltage ripple (ΔV_{out}) and capacitor currents (i_{Crms})) and, finally, a good distribution of semiconductor losses (which is very important regarding the lifetime of the converter [136]).

The proposed simulation scheme (Fig. 10) consists of a three-phase input source 1, input inductors 1, boost-type three-phase rectifier topology under test 4 ($3\theta - 2L$, NPC, Vienna 6-switch, Vienna 3-switch and Vienna T-type), output capacitors 4 and resistive load simulating battery current-demand 5. The test setup is described in Table 7, where the parameter values of the simulation models are detailed.[4,5]

Simulation results are summarized in Table 8. $3\theta - 2L$ topology presents the lowest component count with only six semiconductors, but voltage rating of each one of them is the entire bus voltage,V_{BUS}. The Vienna 3-switch is the topology with the highest component count (21). Regarding efficiency, the $3\theta - 2L$, the Vienna 6-switch and the Vienna T-type present the highest efficiency with values greater

[4]The SKKD8112 diodes can only be used in Vienna 6-switch (Fig. 9(c)) and Vienna 3-switch (Fig. 9(d)) topologies, since the input diodes ($D_1, D_{1'}, D_2, D_{2'}, D_3, D_{3'}$) in these topologies do not switch current at high frequency. With the implementation of these diodes at the input, conduction losses are greatly improved due to their low resistance.

[5]Silicon Carbide (SiC) MOSFET semiconductors has been used to carry out the simulations, since they have better switching performance compared to the Silicon (Si) devices [51]. In this sense, increasing the switching frequency is a suitable technique to reduce the size of the reactive components, thus improving the power density of the converters.

TABLE 8. Comparison table for 50 kW rectifier (switching frequency 100 kHz).

		$3\theta-2L$	NPC	Vienna-6 sw.	Vienna-3 sw.	T-type
Performance and quality						
Hardware	$Diodes$	0	6	12	18	6
	$Switches$	6	12	6	3	6
	$V_{AK}\ (V)$	V_{BUS}	$V_{BUS}/2$	$V_{BUS}/2$	$V_{BUS}/2$	V_{BUS}
	$V_{DS}\ (V)$	V_{BUS}	$V_{BUS}/2$	$V_{BUS}/2$	$V_{BUS}/2$	$V_{BUS}/2$
Performance	$Efficiency\ (\%)$	97.87	96.20	97.38	97.09	97.14
	$Total\ losses\ (W_{avg})$	1062	1896	1308	1455	1428
Input quality	$PF\ (\%)$	99.933	99.992	99.991	99.992	99.992
	$THD\ (\%)$	4.04	1.27	1.26	1.26	1.25
	$cos(\Phi)$	1	1	1	1	1
Output quality	$\Delta V_{BUS}\ (V)$	3.40	4.81	3.26	4.02	1.99
	$i_{Crms}\ (A)$	43.6	47.1	46.7	46.9	42.7

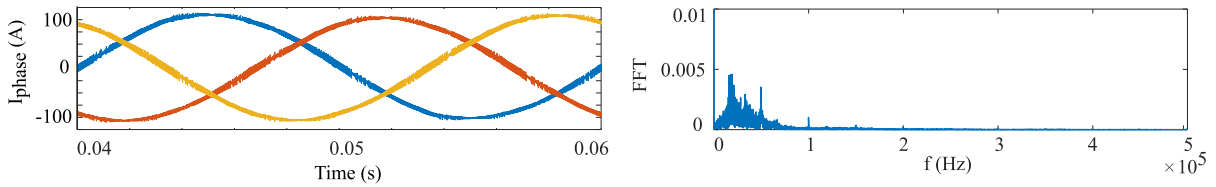

(a) Conventional three-phase two-level ($3\theta-2L$).

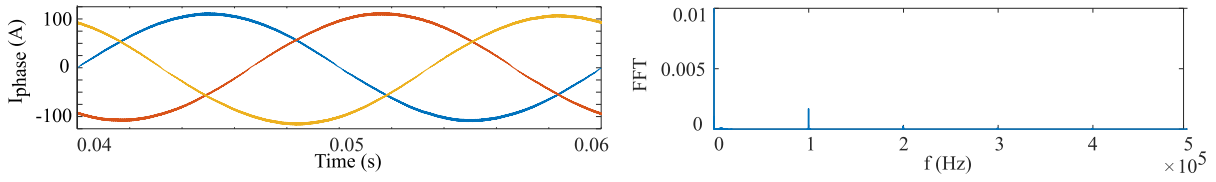

(b) Neutral Point Clamped converter (NPC).

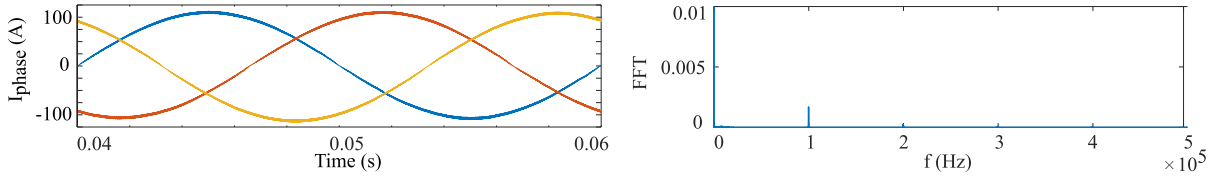

(c) Vienna 6-switch.

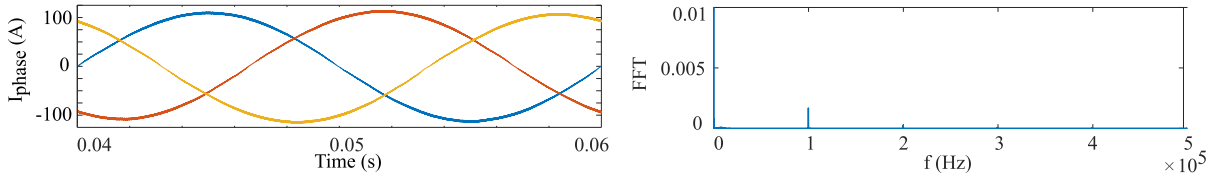

(d) Vienna 3-switch.

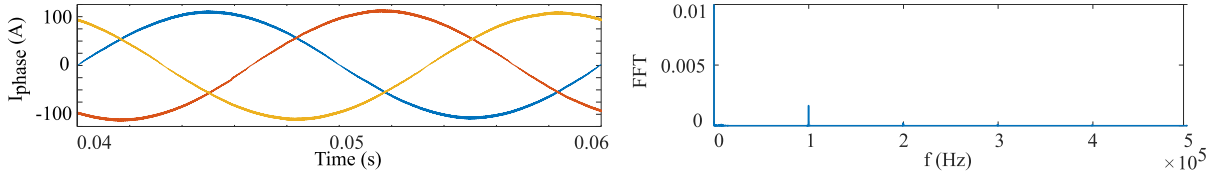

(e) Vienna T-type.

FIGURE 11. Input current waveforms and unity-normalized frequency response (FFT) for compared topologies.

than 96 %. The input current and output voltage waveforms in all the converters ($THD_i < 5\%$, $\Delta V_{BUS} < 4.81\ V$ and $i_{Crms} \in (42.7\ A, 47.1\ A)$ are of high quality, and any of these topologies is valid to achieve the figures of merit required by fast-chargers. Even so, comparing the input current and normalized frequency response (FFT) (Fig. 11), it can be observed that compared to three-level topologies, the $3\theta-2L$ has worse input current quality, as it has the highest

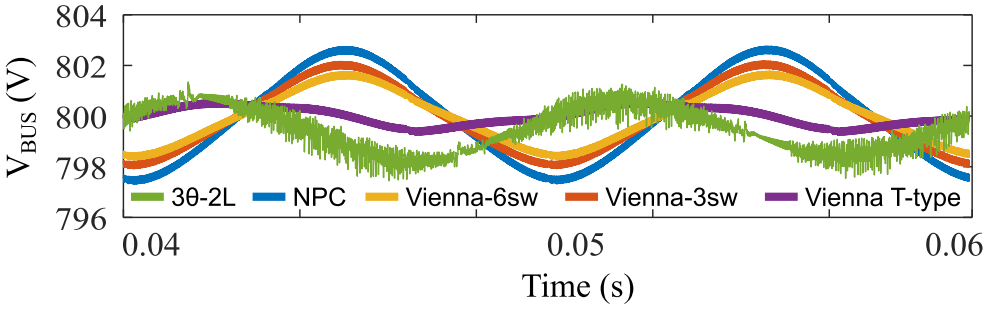

FIGURE 12. Output voltage waveforms V_{BUS} (V).

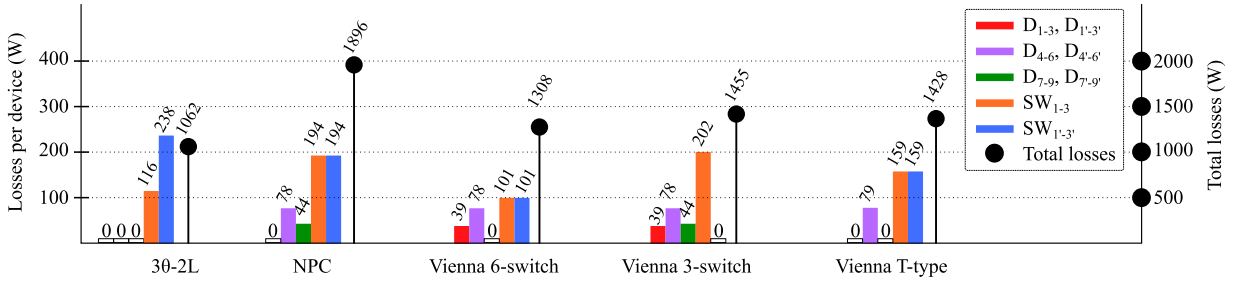

(a) Power loss per device.

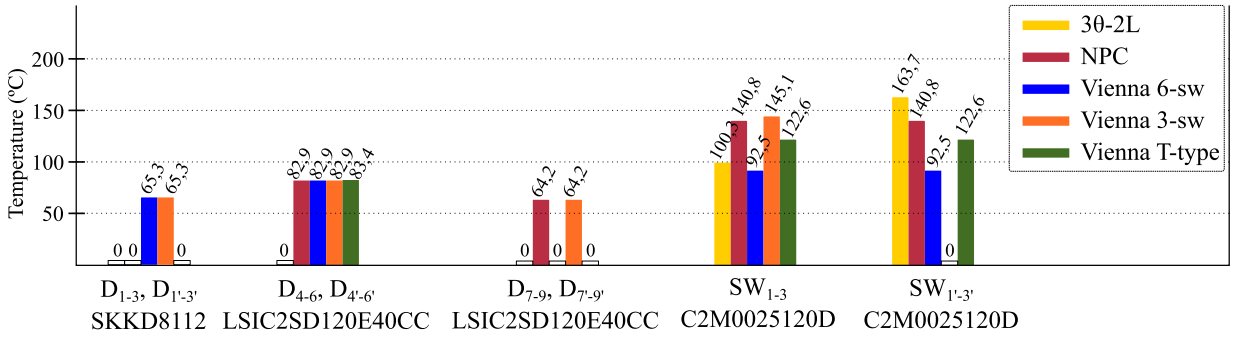

(b) Junction temperature (Tj) per device.

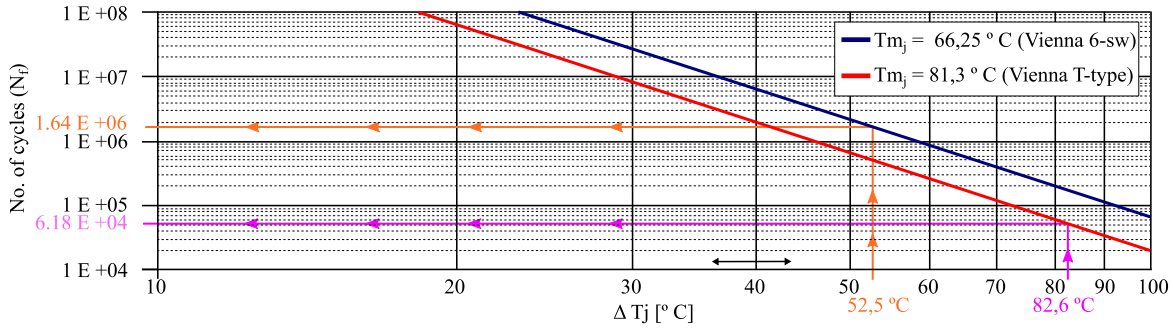

(c) MOSFET lifetime estimation based on LESIT study [137]..

Notes:

a Columns with value '0' means that there are no temperature variations, since the devices do not exist in these topologies.

b Values are obtained by using $Rth_{hs-a} = 0.2\ ^oC/W$, $Rth_{c-hs} = 0.05\ ^oC/W$ and $R_{\theta JC}$ for each type of device (SKKD8112 - $R_{\theta JC} = 0.40\ ^oC/W$, LSIC2SD120E40CC - $R_{\theta JC} = 0.30\ ^oC/W$, C2M0025120D - $R_{\theta JC} = 0.27\ ^oC/W$) and ambient temperature (T_a) of 40 ^oC.

FIGURE 13. Comparison of power losses and temperature increments.

high-frequency current ripple (4 A) and the highest levels of distortion ($THD_i = 4,04$ %). The latter confirms the negative aspect of the two-level voltage converters [120], [121].

Fig. 13(a) shows that distribution of losses is very different for each of the topologies. The first thing that stands out is that the Vienna 6-switch and the Vienna T-type topologies have

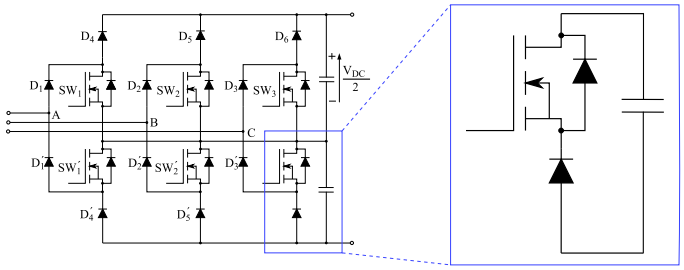

(a) Vienna 6-switch commutation cell.

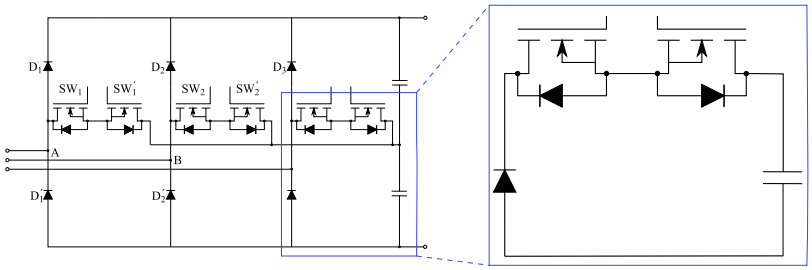

(b) Vienna T-switch commutation cell.

FIGURE 14. **Commutation-cell comparison: entire topology and cell zoom-in.**

better distribution of losses, the former being the one that obtains the best results (101 W [P_{ref}]) compared to the latter (159 $W \equiv P_{ref} + 58\ W$). Conversely, the higher power loss concentration (manly on the MOSFETs) are in the $3\theta - 2L$ (238 $W \equiv P_{ref} + 137\ W$), the NPC (194 $W \equiv P_{ref} + 235\ W$) and the Vienna 3-switch (202 $W \equiv P_{ref} + 101\ W$) converters.

Distribution of losses among semiconductors is a very relevant aspect for the reliability of the converter. One of the most extended model for the estimation of lifetime of semiconductors is the Arrhenius and Coffin-Manson combination [136] of laws of degradation (2),

$$N_f = A\ \Delta Tj\ e^{(Q/R_{gas}T_m)} \tag{2}$$

where A, and α are device dependent constants, R_{gas} is the gas constant (8.314 $J/mol.K$), $Tm_j = T_{jmin} + (T_{jmax} - T_{jmin})/2$ is the mean cycle temperature expressed in Kelvin, and the internal energy Q is $7.8{\times}10^4\ Jmol^{-l}$. ΔTj is the variation of the junction temperature. The constants $\alpha = -5$, and, A=640 are obtained from curve fitting in the LESIT study.

Fig. 13(b) shows the temperature change for each vehicle charge using the same semiconductor device in the five topologies. As shown in Fig. 13(b), the differences in temperature that occur in the diodes are practically negligible. The biggest differences occur in the MOSFETs. In this sense the $3\theta - 2L$, the NPC and the Vienna 3-switch topologies have respectively 163,7 ^oC, 140,8 ^oC and 145,1 ^oC junction temperature (T_j) excursion, which makes these topologies very sensitive regarding lifetime compared to the Vienna 6-switch and Vienna T-type topologies that have respectively 92,5 ^oC and 122,6 ^oC. Regarding the loss distribution, topologies with best thermal behaviour are the Vienna 6-switch and the Vienna T-type, with a maximum temperature deviation between devices of 27,2 ^oC and 39,2 ^oC, respectively.

In order to analyse how much this increase in temperature affects lifetime, LESIT study curves have been chosen (see Fig. 13(c)) to show an approximation of how a few degrees of temperature can vary the lifetime of a device. In this analysis, referring to a 50 kW charging system, it can be seen that the MOSFETs of the Vienna 6-switch can last 1.64 E+06 cycles. Conversely, for the Vienna T-type this number is reduced to 6.18 E + 04. The number of cycles would be much lower in the other three topologies.

According to the defined comparison criteria, the Vienna 6-switch and the Vienna T-type are the best alternative, due to their high efficiency, good quality of input currents and output voltages, and for their better distribution of losses between semiconductors. Because of the similar performance of both topologies (Vienna 6-switch and Vienna T-type), an additional aspect has been considered to make a more accurate comparison, the scalability in switching frequency of the rectifiers. This aspect is relevant since there is a trend towards power converters with higher power densities. In this sense, one of the ways to achieve this is by reducing inductances and capacities by increasing the switching frequency. The Vienna 6-switch high-frequency commutation-cell consists of a single MOSFET and a diode (Fig. 14(a)). On the other side, Vienna T-type (Fig. 14(b)) has to commutate two MOSFETs in series that work as a bidirectional switch. In this sense, series connection on the T-type topology results in an increase in resistive and parasitic components such as inductances, which will cause greater power losses and overshoots in voltage and current. Additionally, this effect can be increased if discrete devices are used instead of modules, since they have higher values of parasitic inductances because of their packaging [137]–[139]. Due to the structure of the Vienna 6-switch, the commutation-cell area is reduced

with the use of a snubber capacitor very near commutation-cell. The result of using these cells have been demonstrated in several works [140]–[142], where commutation cells of about 6 nH are implemented. Moreover, the effectiveness of using snubber capacitors has been also demonstrated in other works [143], [144], reducing switching losses produced by parasitic overshoots on voltage.

The general review and subsequent comparative of electric vehicle charging topologies has concluded with five valid topologies for the EV charging application. Therefore, taking into account the analysis carried out, the most appropriate converters for the application of electric vehicle charging are the Vienna 6-switch and the Vienna T-type, especially for their efficiency, input power quality and stability of the output voltage, all with a suitable distribution of the losses between devices.

VI. CONCLUSION

There is a growing turned towards implementation of policies to reduce the GHG emissions, where the EVs have crucial relevance. Battery systems have a special relevance in EV and that is why short-term improvements have been analysed. In this context, lithium batteries currently are the prevailing technology, and according to the literature they will continue to be so, since these batteries improve the energy density the most (which is expected to double to 1000 Wh/l), increase the number of charging cycles (which will triple the current batteries lifetime), and reduce the price of battery systems (which is expected to be below $ 61/kWh, compared to current prices of $ 156/kWh). Regarding operating voltages, nowadays, most of the EV propulsion systems works at 300-420 V, but the trend is to increase these voltage levels to 800 V. With this trend-change, a reduction on the system current is achieved, making it possible to reduce the wire gauge, thus reducing the weight. It has also been seen that fast-charging users normally only demand power from the grid. In this context, single phase rectifiers require very high currents and would not be able to provide sufficient power levels for fast-charging. Therefore, it is necessary to use three-phase converters, with which the problem of power and high current at the input of the fast-charging rectifiers is solved.

Five suitable topologies ($3\theta - 2L$, the NPC, the Vienna 6-switch, the Vienna 3-switch and the Vienna T-type) have been analysed that improve the current situation of the fast-charging stations of the EVs. Although with some shortcomings, all the presented topologies meet the criteria established in this work, where specially the Vienna 6-switch and the Vienna T-type have an advantage over the other due to their performance, particularly in efficiency, quality of the input currents and output voltages, and in the distribution of losses. Using LESIT study results, it has been shown that small increases in operating temperature can greatly reduce the lifetime of semiconductors and it is important to use designs in which the power losses are distributed between devices.

Finally, it is shown that increasing the switching frequency is feasible in order to reduce passive components, such as coils and capacitors, thus improving the power density of the converters. In this context, it is pointed out that using the Vienna 6-switch rectifier has advantages with respect to scalability in switching frequency, since it has a better commutation-cell if compared to Vienna T-type, the closest rival in the comparison.

REFERENCES

[1] "2050 long-term strategy," Eur. Commission, Brussels, Belgium, Tech. Rep., 2018.
[2] "Global EV outlook," Int. Energy Agency (IEA), Paris, France, Tech. Rep., 2020.
[3] "Inventory of U.S. Greenhousegas emissions and sinks: 1990–2015," United States Environmental Protection Agency (EPA), Washington, DC, USA, Tech. Rep., 2017.
[4] "World population prospects: The 2017 revision," United Nations, New York, NY, USA, Tech. Rep., 2018.
[5] "Annual energy outlook," U.S. Energy Infomation Admin., Washington, DC, USA, Tech. Rep., 2018.
[6] F. Un-Noor, S. Padmanaban, L. Mihet-Popa, M. N. Mollah, and E. Hossain, "A comprehensive study of key electric vehicle (EV) components, technologies, challenges, impacts, and future direction of development," *Energies*, vol. 10, no. 8, p. 1217, 2017.
[7] L. Kumar and S. Jain, "Electric propulsion system for electric vehicular technology: A review," *Renew. Sustain. Energy Rev.*, vol. 29, pp. 924–940, Jan. 2014.
[8] "Electric vehicle initiative," Clean Energy Ministerial (CEM), Paris, France, Tech. Rep., 2019.
[9] "2030 global electrified vehicle outlook," Energy Inst. Univ. Michigan, Ann Arbor, MI, USA, Tech. Rep., 2019.
[10] "EV100 progress and insights report," The Climate Group, New York, NY, USA, Tech. Rep., 2020.
[11] "GEF-7 strategy," Global Enrironment Facility (GEF), Washington, DC, USA, Tech. Rep., 2019.
[12] I. López, E. Ibarra, A. Matallana, J. Andreu, and I. Kortabarria, "Next generation electric drives for HEV/EV propulsion systems: Technology, trends and challenges," *Renew. Sustain. Energy Rev.*, vol. 114, Oct. 2019, Art. no. 109336.
[13] "3-phase AC-DC seminar," Infineon Technol., Neubiberg, Germany, Tech. Rep., 2020.
[14] H. S. Das, M. M. Rahman, S. Li, and C. W. Tan, "Electric vehicles standards, charging infrastructure, and impact on grid integration: A technological review," *Renew. Sustain. Energy Rev.*, vol. 120, Mar. 2020, Art. no. 109618.
[15] J. Y. Yong, V. K. Ramachandaramurthy, K. M. Tan, and N. Mithulananthan, "A review on the state-of-the-art technologies of electric vehicle, its impacts and prospects," *Renew. Sustain. Energy Rev.*, vol. 49, pp. 365–385, Sep. 2015.
[16] C. C. Chan, "The state of the art of electric, hybrid, and fuel cell vehicles," *Proc. IEEE*, vol. 95, no. 4, pp. 704–718, Apr. 2007.
[17] K. V. Singh, H. O. Bansal, and D. Singh, "A comprehensive review on hybrid electric vehicles: Architectures and components," *J. Mod. Transport.*, vol. 27, pp. 77–107, Jun. 2019.
[18] M. Yilmaz and P. T. Krein, "Review of battery charger topologies, charging power levels, and infrastructure for plug-in electric and hybrid vehicles," *IEEE Trans. Power Electron.*, vol. 28, no. 5, pp. 2151–2169, May 2013.
[19] Z. Li, A. Khajepour, and J. Song, "A comprehensive review of the key technologies for pure electric vehicles," *Energy*, vol. 182, pp. 824–839, Sep. 2019.
[20] T. Chen, X. Zhang, J. Wang, J. Li, C. Wu, M. Hu, and H. Bian, "A review on electric vehicle charging infrastructure development in the UK," *J. Modern Power Syst. Clean Energy*, vol. 8, no. 2, pp. 193–205, 2020.
[21] B. W. M. Woodward and J. Hamilton, "Electric vehicles—Setting a course for 2030," Deloitte Insights, New York, NY, USA, Tech. Rep., 2020.
[22] "Voltage classes for electric mobility," ZVEI, Die Elektroindustrie, Frankfurt, Germany, Tech. Rep., 2013.

[23] C. Jung, "Power up with 800-V systems: The benefits of upgrading voltage power for battery-electric passenger vehicles," *IEEE Electrific. Mag.*, vol. 5, no. 1, pp. 53–58, Mar. 2017.
[24] A. Meintz, J. Zhang, R. Vijayagopal, C. Kreutzer, S. Ahmed, I. Bloom, A. Burnham, R. B. Carlson, F. Dias, E. J. Dufek, and J. Francfort, "Enabling fast charging—Vehicle considerations," *J. Power Sources*, vol. 367, pp. 216–227, Nov. 2017.
[25] V. Reber, "New possibilities with 800-volt charging," *Porsche Eng. Mag.*, vol. 1, pp. 10–15, Jan. 2020.
[26] A. Engstle, M. Deiml, A. Angermaier, and W. Schelter, "800 volt for electric vehicles voltage level suitable for calibration," *ATZ Worldwide*, vol. 115, no. 9, pp. 38–43, Sep. 2013.
[27] R. W. D. Doncker, "Fast charging (350 kw) for electric vehicles—Possibilities and issues," *Seminar*, to be published.
[28] B. Nykvist and M. Nilsson, "Rapidly falling costs of battery packs for electric vehicles," *Nature Climate Change*, vol. 5, no. 4, pp. 329–332, 2015.
[29] S. I. Sun, A. J. Chipperfield, M. Kiaee, and R. G. A. Wills, "Effects of market dynamics on the time-evolving price of second-life electric vehicle batteries," *J. Energy Storage*, vol. 19, pp. 41–51, Oct. 2018.
[30] M. Gjelaj, S. Hashemi, C. Traeholt, and P. B. Andersen, "Grid integration of DC fast-charging stations for EVs by using modular li-ion batteries," *IET Gener., Transmiss. Distrib.*, vol. 12, no. 20, pp. 4368–4376, Nov. 2018.
[31] L. Yang and H. Ribberink, "Investigation of the potential to improve DC fast charging station economics by integrating photovoltaic power generation and/or local battery energy storage system," *Energy*, vol. 167, pp. 246–259, Jan. 2019.
[32] M. M. Mahfouz and M. R. Iravani, "Grid-integration of battery-enabled DC fast charging station for electric vehicles," *IEEE Trans. Energy Convers.*, vol. 35, no. 1, pp. 375–385, Mar. 2020.
[33] E. Garcia and I. Isaac, "Demand response systems for integrating energy storage batteries for residential users," in *Proc. IEEE Ecuador Tech. Chapters Meeting (ETCM)*, Oct. 2016, pp. 1–6.
[34] P. Denholm, J. Nunemaker, P. Gagnon, and W. Cole, "The potential for battery energy storage to provide peaking capacity in the united states," *Renew. Energy*, vol. 151, pp. 1269–1277, May 2020.
[35] D. Stenclik, B. Zhang, R. Rocheleau, and J. Cole, "Energy storage as a peaker replacement: Can solar and battery energy storage replace the capacity value of thermal generation?" *IEEE Electrific. Mag.*, vol. 6, no. 3, pp. 20–26, Sep. 2018.
[36] R. Yokoyama, Y. Hida, K. Koyanagi, and K. Iba, "The role of battery systems and expandable distribution networks for smarter grid," in *Proc. IEEE Power Energy Soc. Gen. Meeting*, Jul. 2011, pp. 1–6.
[37] Y. Zhang, A. Melin, M. Olama, S. Djouadi, J. Dong, and K. Tomsovic, "Battery energy storage scheduling for optimal load variance minimization," in *IEEE Power Energy Soc. Innov. Smart Grid Technol. Conf. (ISGT)*, 2018, pp. 1–5.
[38] "Electricity storage and renewables: Costs and markets to 2030," IRENA, Abu Dhabi, United Arab Emirates, Tech. Rep., 2017.
[39] "Smart charging for electric vehicles," Int. Renew. Energy Agency (IRENA), Abu Dhabi, United Arab Emirates, Tech. Rep., 2019.
[40] "Battery innovation roadmap 2030," Assoc. Eur. Automot. Ind. Battery Manufacturers (EUROBAT), Rumia, Poland, Tech. Rep., 2019.
[41] X. Tian, Y. Wu, P. Hou, S. Liang, S. Qu, M. Xu, and T. Zuo, "Environmental impact and economic assessment of secondary lead production: Comparison of main spent lead-acid battery recycling processes in China," *J. Cleaner Prod.*, vol. 144, pp. 142–148, Feb. 2017.
[42] M. Caruso, V. Castiglia, R. Miceli, C. Nevoloso, P. Romano, G. Schettino, F. Viola, M. G. Insinga, A. Moncada, R. L. Oliveri, F. Ganci, C. Sunseri, S. Piazza, and R. Inguanta, "Nanostructured lead acid battery for electric vehicles applications," in *Proc. Int. Conf. Electr. Electron. Technol. Automot.*, Jun. 2017, pp. 1–5.
[43] U. Akram, M. Nadarajah, R. Shah, and F. Milano, "A review on rapid responsive energy storage technologies for frequency regulation in modern power systems," *Renew. Sustain. Energy Rev.*, vol. 120, Mar. 2020, Art. no. 109626.
[44] X. Fan, B. Liu, J. Liu, J. Ding, X. Han, Y. Deng, X. Lv, Y. Xie, B. Chen, W. Hu, and C. Zhong, "Battery technologies for grid-level large-scale electrical energy storage," *Trans. Tianjin Univ.*, vol. 26, no. 2, pp. 92–103, Apr. 2020.
[45] M. A. Hannan, M. M. Hoque, A. Mohamed, and A. Ayob, "Review of energy storage systems for electric vehicle applications: Issues and challenges," *Renew. Sustain. Energy Rev.*, vol. 69, pp. 771–789, Mar. 2017.
[46] M. A. Hannan, M. M. Hoque, A. Hussain, Y. Yusof, and P. J. Ker, "State-of-the-art and energy management system of lithium-ion batteries in electric vehicle applications: Issues and recommendations," *IEEE Access*, vol. 6, pp. 19362–19378, 2018.
[47] D.-I. Stroe, V. Knap, M. Swierczynski, A.-I. Stroe, and R. Teodorescu, "Operation of a grid-connected lithium-ion battery energy storage system for primary frequency regulation: A battery lifetime perspective," *IEEE Trans. Ind. Appl.*, vol. 53, no. 1, pp. 430–438, Jan./Feb. 2017.
[48] U. K. Das, P. Shrivastava, K. S. Tey, M. Y. I. Bin Idris, S. Mekhilef, E. Jamei, M. Seyedmahmoudian, and A. Stojcevski, "Advancement of lithium-ion battery cells voltage equalization techniques: A review," *Renew. Sustain. Energy Rev.*, vol. 134, Dec. 2020, Art. no. 110227.
[49] P. T. Moseley, D. A. J. Rand, J. Garche, J. Garche, E. Karden, P. T. Moseley, and D. A. J. Rand, "Lead-acid batteries for future automobiles: Status and prospects," in *Lead-Acid Batteries for Future Automobiles*. Amsterdam, The Netherlands: Elsevier, 2017, pp. 601–618.
[50] "Electric vehicle outlook 2020," BloombergNEF, London, U.K., Tech. Rep., 2020.
[51] A. Matallana, E. Ibarra, I. López, J. Andreu, J. I. Garate, X. Jorda, and J. Rebollo, "Power module electronics in HEV/EV applications: New trends in wide-bandgap semiconductor technologies and design aspects," *Renew. Sustain. Energy Rev.*, vol. 113, Oct. 2019, Art. no. 109264.
[52] M.-H. Lu and M. Jen, "Safety design of electric vehicle charging equipment," *World Electric Vehicle J.*, vol. 5, no. 4, pp. 1017–1024, Dec. 2012.
[53] V. Prasanth, D. Foley, and S. Ravi, "Demystifying automotive safety and security for semiconductor developer," in *Proc. IEEE Int. Test Conf. (ITC)*, Oct. 2017, pp. 1–10.
[54] J. Bablo, "Electric vehicle infrastructure standardization," *World Electr. Vehicle J.*, vol. 8, no. 2, pp. 576–586, Jun. 2016.
[55] K. Knezović, S. Martinenas, P. B. Andersen, A. Zecchino, and M. Marinelli, "Enhancing the role of electric vehicles in the power grid: Field validation of multiple ancillary services," *IEEE Trans. Transport. Electrific.*, vol. 3, no. 1, pp. 201–209, Mar. 2017.
[56] "Charging technology for electro-mobility," Phoenix Contact, Blomberg, Germany, Tech. Rep., 2020.
[57] Z. Lin and D. L. Greene, "Promoting the market for plug-in hybrid and battery electric vehicles: Role of recharge availability," *Transp. Res. Rec., J. Transp. Res. Board*, vol. 2252, no. 1, pp. 49–56, Jan. 2011.
[58] M. E. Kabir, C. Assi, H. Alameddine, J. Antoun, and J. Yan, "Demand aware deployment and expansion method for an electric vehicles fast charging network," in *Proc. IEEE Int. Conf. Commun., Control, Comput. Technol. Smart Grids (SmartGridComm)*, Oct. 2019, pp. 1–7.
[59] T. R. Tanim, E. J. Dufek, M. Evans, C. Dickerson, A. N. Jansen, B. J. Polzin, A. R. Dunlop, S. E. Trask, R. Jackman, I. Bloom, Z. Yang, and E. Lee, "Extreme fast charge challenges for lithium-ion battery: Variability and positive electrode issues," *J. Electrochem. Soc.*, vol. 166, no. 10, pp. A1926–A1938, 2019.
[60] Y. Cao, O. Kaiwartya, C. Han, K. Wang, H. Song, and N. Aslam, "Toward distributed battery switch based electro-mobility using publish/subscribe system," *IEEE Trans. Veh. Technol.*, vol. 67, no. 11, pp. 10204–10217, Nov. 2018.
[61] X.-G. Yang and C.-Y. Wang, "Understanding the trilemma of fast charging, energy density and cycle life of lithium-ion batteries," *J. Power Sources*, vol. 402, pp. 489–498, Oct. 2018.
[62] F. Sehar, M. Pipattanasomporn, and S. Rahman, "Demand management to mitigate impacts of plug-in electric vehicle fast charge in buildings with renewables," *Energy*, vol. 120, pp. 642–651, Feb. 2017.
[63] P. Morrissey, P. Weldon, and M. O'Mahony, "Informing the strategic roll-out of fast electric vehicle charging networks with user charging behavior data analysis," *Transp. Res. Rec., J. Transp. Res. Board*, vol. 2572, no. 1, pp. 9–19, Jan. 2016.
[64] "American housing survey," Tech. Rep., 2016.
[65] "Learning from norwegian battery electric and plug-in hybrid vehicle users. Results from a survey of vehicle owners," Inst. Transp. Econ., Oslo, Oslo, Norway, Tech. Rep., 2016.
[66] "Electromobility status in norway. Mastering long distances—The last hurdle to mass adoption," Inst. Transp. Econ., Oslo, Oslo, Norway, TOI Tech. Rep. 1627, 2018.
[67] S. Hardman, A. Jenn, G. Tal, J. Axsen, G. Beard, N. Daina, and Figenbaum, "A review of consumer preferences of and interactions with electric vehicle charging infrastructure," *Transp. Res. D, Transp. Environ.*, vol. 62, pp. 508–523, 2018.

[68] J. W. Kolar and T. Friedli, "The essence of three-phase PFC rectifier systems—Part I," *IEEE Trans. Power Electron.*, vol. 28, no. 1, pp. 176–198, Jan. 2013.
[69] T. Friedli, M. Hartmann, and J. W. Kolar, "The essence of three-phase PFC rectifier systems—Part II," *IEEE Trans. Power Electron.*, vol. 29, no. 2, pp. 543–560, Feb. 2014.
[70] A. Kuperman, U. Levy, J. Goren, A. Zafranski, and A. Savernin, "High power Li-ion battery charger for electric vehicle," in *Proc. 7th Int. Conf. Workshop Compat. Power Electron. (CPE)*, Jun. 2011, pp. 342–347.
[71] S. Kim, P. N. Enjeti, and I. J. Pitel, "A new approach to improve power factor and reduce harmonicsin a three-phase diod rectifier type utility interface," *IEEE Trans. Ind. Appl.*, vol. 30, no. 6, p. 1557, Nov. 1994.
[72] S. Bala, T. Tengner, P. Rosenfeld, and F. Delince, "The effect of low frequency current ripple on the performance of a lithium iron phosphate (LFP) battery energy storage system," in *Proc. IEEE Energy Convers. Congr. Expo. (ECCE)*, Sep. 2012, pp. 3485–3492.
[73] K. Uddin, A. D. Moore, A. Barai, and J. Marco, "The effects of high frequency current ripple on electric vehicle battery performance," *Appl. Energy*, vol. 178, pp. 142–154, Sep. 2016.
[74] V.-S. Nguyen, V.-L. Tran, W. Choi, and D.-W. Kim, "Analysis of the output ripple of the DC–DC boost charger for li-ion batteries," *J. Power Electron.*, vol. 14, no. 1, pp. 135–142, Jan. 2014.
[75] T. B. Soeiro and J. W. Kolar, "Analysis of high-efficiency three-phase Two- and three-level unidirectional hybrid rectifiers," *IEEE Trans. Ind. Electron.*, vol. 60, no. 9, pp. 3589–3601, Sep. 2013.
[76] M. Leibl, J. W. Kolar, and J. Deuringer, "Sinusoidal input current discontinuous conduction mode control of the VIENNA rectifier," *IEEE Trans. Power Electron.*, vol. 32, no. 11, pp. 8800–8812, Nov. 2017.
[77] J. W. Kolar, H. Ertl, and F. C. Zach, "Design and experimental investigation of a three-phase high power density high efficiency unity power factor PWM (VIENNA) rectifier employing a novel integrated power semiconductor module," in *Proc. Appl. Power Electron. Conf.*, vol. 2, Mar. 1996, pp. 514–523.
[78] T. Viitanen and H. Tuusa, "A steady-state power loss consideration of the 50kW VIENNA i and PWM full-bridge three-phase rectifiers," in *Proc. IEEE 33rd Annu. IEEE Power Electron. Spec. Conf.*, Jun. 2002, pp. 915–920.
[79] Q. Wang, X. Zhang, R. Burgos, D. Boroyevich, A. White, and M. Kheraluwala, "Design and implementation of interleaved vienna rectifier with greater than 99% efficiency," in *Proc. IEEE Appl. Power Electron. Conf. Expo. (APEC)*, Mar. 2015, pp. 72–78.
[80] K. Mahmud, L. Tao, and M. S. Alam, "A variable speed three phase generator voltage hook up with a DC bus by VIENNA rectifier," in *Proc. Int. Conf. Electr. Inf. Commun. Technol. (EICT)*, Feb. 2014, pp. 1–6.
[81] X. Zhang, Q. Wang, R. Burgos, and D. Boroyevich, "Discontinuous pulse width modulation methods with neutral point voltage balancing for three phase vienna rectifiers," in *Proc. IEEE Energy Convers. Congr. Exposit. (ECCE)*, Sep. 2015, pp. 225–232.
[82] K. Hirachi, K. Nishimura, N. Baba, L. Gamage, A. Chibani, and M. Nakaoka, "Engine-driven generator interactive three-phase switched-mode PFC converter and its performance evaluations," in *Proc. IEEE Int. Symp. Ind. Electron., (ISIE)*, vol. 2, Jul. 1997, pp. 612–618.
[83] S. M. Ulhaq, "Object-oriented simulation of DSP controlled three phase active PFC converter," in *Proc. 7th Int. Conf. Power Electron. Variable Speed Drives*, 1998, pp. 28–33.
[84] E. Hiraki, M. Yoshida, M. Nakaoka, N. Hatano, and Y. Sugawara, "Feasible evaluations of space vector modulated three-phase soft-switching PFC rectifier with instantaneous power feedback scheme," in *Proc. 5th Int. Conf. Power Electron. Drive Syst. (PEDS)*, Nov. 2003, pp. 1126–1131.
[85] J. Wu, H. Dai, K. Xing, F. C. Lee, and D. Boroyevich, "Implementation of a ZCT soft switching technique in a 100 kW PEBB based three-phase PFC rectifier," in *Proc. 30th Annu. IEEE Power Electron. Spec. Conf. Record.*, Jul. 1999, pp. 647–652.
[86] R. Zhang, F. C. Lee, and D. Boroyevich, "Four-legged three-phase PFC rectifier with fault tolerant capability," in *Proc. IEEE 31st Annu. Power Electron. Spec. Conf.*, Jun. 2000, pp. 359–364.
[87] D. Yazdani, A. R. Bakhshai, H. Norouzzadeh, and T. Abaspour, "Introducing a novel space vector classification technique for performance improvement of a three-phase PFC converters," in *Proc. 5th Int. Conf. Power Electron. Drive Syst. (PEDS)*, Nov. 2003, pp. 582–585.
[88] R. Li, K. Ma, and D. Xu, "A novel 40KW ZVS-SVM controlled three-phase boost PFC converter," in *Proc. 24th Annu. IEEE Appl. Power Electron. Conf. Expo.*, Feb. 2009, pp. 376–382.
[89] Y. Chen and K. M. Smedley, "Parallel operation of one-cycle controlled three-phase PFC rectifiers," *IEEE Trans. Ind. Electron.*, vol. 54, no. 6, pp. 3217–3224, Dec. 2007.
[90] C. Bing, X. Yunxiang, and T. Fei, "A novel three-phase buck PFC converter based on one-cycle control," in *Proc. Int. Conf. Power Syst. Technol.*, Oct. 2006, pp. 1–7.
[91] J.-I. Itoh and I. Ashida, "A novel three-phase PFC rectifier using a harmonic current injection method," *IEEE Trans. Power Electron.*, vol. 23, no. 2, pp. 715–722, Mar. 2008.
[92] B. Huang, R. Burgos, F. Wang, and D. Boroyevich, "D-Q-0 synchronous frame average model for three-phase arrays of single-phase PFC converter loads," in *Proc. IEEE Workshops Comput. Power Electron.*, Jul. 2006, pp. 83–88.
[93] T. Takahara, M. Okamoto, E. Hiraki, T. Tanaka, T. Hashizume, and T. Kachi, "Performance verification of a novel soft switching three-phase utility frequency AC to high frequency AC direct power converter with PFC function for industrial IH applications," in *Proc. 14th Int. Power Electron. Motion Control Conf. (EPE-PEMC)*, Sep. 2010, pp. T6-54–T6-60.
[94] P. Cortes, J. W. Kolar, and J. Rodriguez, "Comparative evaluation of predictive control schemes for three-phase buck-type PFC rectifiers," in *Proc. 7th Int. Power Electron. Motion Control Conf. (IPEMC)*, vol. 1, Jun. 2012, pp. 666–672.
[95] D. F. Cortez and I. Barbi, "A three-phase multilevel hybrid switched-capacitor PWM PFC rectifier for high-voltage-gain applications," *IEEE Trans. Power Electron.*, vol. 31, no. 5, pp. 3495–3505, May 2016.
[96] D. C. Morais, F. J. M. de Seixas, L. C. Souza, L. S. C. e Silva, and J. C. P. Junior, "Three-phase half-controlled boost PFC rectifier with new variable duty cycle control," in *Proc. 13th IEEE Int. Conf. Ind. Appl. (INDUSCON)*, Nov. 2018, pp. 131–137.
[97] D. M. Xu, C. Yang, J. H. Kong, and Z. Qian, "Quasi soft-switching partly decoupled three-phase PFC with approximate unity power factor," in *Proc. 13th Annu. Appl. Power Electron. Conf. Expo., (APEC)*, vol. 2, Feb. 1998, pp. 953–957.
[98] N. Takeuchi, K. Matsui, I. Yamamoto, M. Hasegawa, F. Ueda, and H. Mori, "A novel PFC circuit for three-phase utilizing a single switching device," in *Proc. INTELEC IEEE 30th Int. Telecommun. Energy Conf.*, Sep. 2008, pp. 1–5.
[99] K. Yao, C. Zou, Z. Ye, and X. Ruan, "Three-phase single-switch boost power factor correction converter with high input power factor," *IET Power Electron.*, vol. 5, no. 7, pp. 1095–1103, Aug. 2012.
[100] Y. Jang and M. M. Jovanović, "The TAIPEI rectifier—A new three-phase two-switch ZVS PFC DCM boost rectifier," *IEEE Trans. Power Electron.*, vol. 28, no. 2, pp. 686–694, Feb. 2013.
[101] N.-V. Olarescu, M.-C. Ancuti, C. Sorandaru, S. Musuroi, M. Svoboda, A. Hedes, D. Popovici, and M. Wienmann, "Performances/efficiency analysis for high efficiency three-phase buck-type PFC rectifiers," in *Proc. 17th Eur. Conf. Power Electron. Appl. (EPE ECCE-Eur.)*, Sep. 2015, pp. 1–9.
[102] M.-C. Ancuti, C. Sorandaru, S. Musuroi, and V.-N. Olarescu, "High efficiency three-phase interleaved buck-type PFC rectifier concepts," in *Proc. IECON 41st Annu. Conf. IEEE Ind. Electron. Soc.*, Nov. 2015, pp. 004990–004995.
[103] M.-C. Ancuti, V.-N. Olarescu, C. Sorandaru, and S. Musuroi, "Performances of the eight-switch versus interleaved eight-switch three-phase buck-type PFC rectifiers," in *Proc. Int. Aegean Conf. Electr. Mach. Power Electron. (ACEMP), Int. Conf. Optim. Electr. Electron. Equip. (OPTIM) Int. Symp. Adv. Electromech. Motion Syst. (ELECTROMOTION)*, Sep. 2015, pp. 382–387.
[104] M. W. Albader and P. Enjeti, "A modular three phase power factor correction (PFC) approach with two single phase PFC stages and an electronic phase shifter," in *Proc. IEEE Appl. Power Electron. Conf. Expo. (APEC)*, Mar. 2015, pp. 79–83.
[105] A. H. Abedin, K. L. Bashar, S. Islam, and M. A. Choudhury, "Output regulated one-switch three-phase boost and boost-buck (SEPIC) PFC rectifiers," in *Proc. IEEE Int. Conf. Power Syst. Technol. (POWERCON)*, Sep. 2016, pp. 1–6.
[106] S. Ali and J. Mutale, "Reactive power management at transmission/distribution interface," in *Proc. 50th Int. Universities Power Eng. Conf. (UPEC)*, Sep. 2015, pp. 1–6.
[107] X. Huang and X. Zhang, "A novel three-phase single-stage PFC converter with limited double-polarity control," in *Proc. IECON - 43rd Annu. Conf. IEEE Ind. Electron. Soc.*, Oct. 2017, pp. 4088–4093.

[108] J. W. Kolar and T. Friedli, "The essence of three-phase PFC rectifier systems," in *Proc. IEEE 33rd Int. Telecommun. Energy Conf. (INTELEC)*, Oct. 2011, pp. 1–27.

[109] C. Qiao and K. M. Smedley, "A general three-phase PFC controller for rectifiers with a series-connected dual-boost topology," *IEEE Trans. Ind. Appl.*, vol. 38, no. 1, pp. 137–148, Jan. 2002.

[110] C. Qiao and K. M. Smedley, "A general three-phase PFC controller for rectifiers with a parallel-connected dual boost topology," *IEEE Trans. Power Electron.*, vol. 17, no. 6, pp. 925–934, Nov. 2002.

[111] L. Zhou, X. Du, Q. Luo, and L. Ran, "A new high efficiency three-phase boost type PFC circuit with integration reset control," in *Proc. 30th Annu. Conf. Ind. Electron. Soc. (IECON)*, vol. 1, Nov. 2004, pp. 790–795.

[112] A. Stupar, T. Friedli, J. Miniböck, and J. W. Kolar, "Towards a 99% efficient three-phase buck-type PFC rectifier for 400-V DC distribution systems," *IEEE Trans. Power Electron.*, vol. 27, no. 4, pp. 1732–1744, Apr. 2012.

[113] L. Hang, M. Zhang, L. M. Tolbert, and Z. Lu, "Digitized feedforward compensation method for high-power-density three-phase Vienna PFC converter," *IEEE Trans. Ind. Electron.*, vol. 60, no. 4, pp. 1512–1519, Apr. 2013.

[114] L. Wang, D. Zhang, Y. Wang, and Y. Gu, "Dynamic performance optimization for high-power density three-phase vienna PFC rectifier," in *Proc. IEEE 2nd Int. Future Energy Electron. Conf. (IFEEC)*, Nov. 2015, pp. 1–4.

[115] M. N. Uddin, A. H. Abedin, K. L. Bashar, S. Islam, and M. A. Choudhury, "Three phase one switch modular-boost/vienna power factor corrected (PFC) rectifier," in *Proc. IEEE Int. Conf. Ind. Technol. (ICIT)*, Mar. 2017, pp. 230–235.

[116] L. Schrittwieser, J. W. Kolar, and T. B. Soeiro, "99efficient three-phase buck-type SiC MOSFET PFC rectifier minimizing life cycle cost in DC data centers," *CPSS Trans. Power Electron. Appl.*, vol. 2, no. 1, pp. 47–58, 2017.

[117] Q. Wang, X. Zhang, R. Burgos, D. Boroyevich, A. M. White, and M. Kheraluwala, "Design and implementation of a two-channel interleaved vienna-type rectifier with >99% efficiency," *IEEE Trans. Power Electron.*, vol. 33, no. 1, pp. 226–239, Jan. 2018.

[118] S. P. Prakash, R. Kalpana, B. Singh, and G. Bhuvaneswari, "Design and implementation of sensorless voltage control of front-end rectifier for power quality improvement in telecom system," *IEEE Trans. Ind. Appl.*, vol. 54, no. 3, pp. 2438–2448, May/Jun. 2018.

[119] E. S. Kim, Y. B. Byun, M. H. Kye, K. Y. Joe, H. H. Koo, Y. H. Kim, and B. D. Yoon, "A leading current compensation control in three phase PWM AC/DC converter," in *Proc. Intelec96 Int. Telecommun. Energy Conf.*, Oct. 1996, pp. 556–561.

[120] M. Annoukoubi, A. Essadki, H. Laghridat, and T. Nasser, "Comparative study between the performances of a three-level and two-level converter for a wind energy conversion system," in *Proc. Int. Conf. Wireless Technol., Embedded Intell. Syst. (WITS)*, Apr. 2019, pp. 1–6.

[121] M. Z. Sujod and I. Erlich, "Harmonics and common mode voltage in a DFIG with two-level and three-level NPC converter using standard PWM techniques," in *Proc. IECON 39th Annu. Conf. IEEE Ind. Electron. Soc.*, Nov. 2013, pp. 1650–1655.

[122] R. H. Baker, "Bridge converter circuit," U.S. Patent 4 270 163 A, May 26, 1981.

[123] M. Stempfle, M. Fischer, M. Nitzsche, J. Wolfle, and J. Roth-Stielow, "Efficiency analysis of three-level NPC and T-type voltage source inverter for various operation modes optimizing the overall drive train efficiency by an operating mode selection," in *Proc. 18th Eur. Conf. Power Electron. Appl. (EPE ECCE Eur.)*, Sep. 2016, pp. 1–10.

[124] C. Roncero-Clemente, E. Romero-Cadaval, V. F. Pires, J. F. Martins, N. Vilhena, and O. Husev, "Efficiency and loss distribution analysis of the 3L-active NPC qZS inverter," in *Proc. IEEE 12th Int. Conf. Compat., Power Electron. Power Eng. (CPE-POWERENG)*, Apr. 2018, pp. 1–6.

[125] W. Phipps, R. T. Harris, and A. G. Roberts, "New generation three-phase rectifier," *SAIEE Afr. Res. J.*, vol. 100, no. 3, pp. 62–67, Sep. 2009.

[126] L. Ma, T. Kerekes, P. Rodriguez, X. Jin, R. Teodorescu, and M. Liserre, "A new PWM strategy for grid-connected half-bridge active NPC converters with losses distribution balancing mechanism," *IEEE Trans. Power Electron.*, vol. 30, no. 9, pp. 5331–5340, Sep. 2015.

[127] R. Katebi, J. He, T. A. Bobeck, W. A. Khan, and N. Weise, "High-efficiency fault-tolerant three-level SiC active NPC converter for safety-critical renewable energy applications," in *Proc. IEEE 10th Int. Symp. Power Electron. Distrib. Gener. Syst. (PEDG)*, Jun. 2019, pp. 665–669.

[128] Z. Hao, H. Bing, Q. Kewang, L. Yan, and T. Chaonan, "The efficiency analysis for three-level grid-connected photovoltaic inverters," in *Proc. IEEE Int. Symp. Ind. Electron.*, May 2012, pp. 1086–1090.

[129] B. Guo, F. Wang, and E. Aeloiza, "A novel three-phase current source rectifier with delta-type input connection to reduce the device conduction loss," *IEEE Trans. Power Electron.*, vol. 31, no. 2, pp. 1074–1084, Feb. 2016.

[130] P. Grzejszczak, A. Kulpa, and R. Barlik, "Design of a high-efficiency three-phase three-level NPC converter based on GaN HEMT and SiC SB diode," in *Proc. Prog. Appl. Electr. Eng. (PAEE)*, Jun. 2019, pp. 1–6.

[131] R. Teichmann and S. Bernet, "A comparison of three-level converters versus two-level converters for low-voltage drives, traction, and utility applications," *IEEE Trans. Ind. Appl.*, vol. 41, no. 3, pp. 855–865, May 2005.

[132] T. Bruckner, S. Bernet, and H. Guldner, "The active NPC converter and its loss-balancing control," *IEEE Trans. Ind. Electron.*, vol. 52, no. 3, pp. 855–868, Jun. 2005.

[133] J. Rodriguez, S. Bernet, P. K. Steimer, and I. E. Lizama, "A survey on neutral-point-clamped inverters," *IEEE Trans. Ind. Electron.*, vol. 57, no. 7, pp. 2219–2230, Jul. 2010.

[134] J. W. Kolar and F. C. Zach, "A novel three-phase utility interface minimizing line current harmonics of high-power telecommunications rectifier modules," *IEEE Trans. Ind. Electron.*, vol. 44, no. 4, pp. 456–467, Aug. 1997.

[135] J. Holtz, "Self-commutated three-phase inverters with staircase voltage-waveforms for high-power applications at low switching frequency," *Siemens Res. Dev. Rep*, vol. 6, no. 3, pp. 164–171, 1977.

[136] M. Held, P. Jacob, G. Nicoletti, P. Scacco, and M.-H. Poech, "Fast power cycling test of IGBT modules in traction application," in *Proc. 2nd Int. Conf. Power Electron. Drive Syst.*, vol. 1, May 1997, pp. 425–430.

[137] K. Aikawa, T. Shiida, R. Matsumoto, K. Umetani, and E. Hiraki, "Measurement of the common source inductance of typical switching device packages," in *Proc. IEEE 3rd Int. Future Energy Electron. Conf. ECCE Asia (IFEEC–ECCE Asia)*, Jun. 2017, pp. 1172–1177.

[138] F. Denk, K. Haehre, S. Eizaguirre Cabrera, C. Simon, M. Heidinger, R. Kling, and W. Heering, "R DS(on) vs. Inductance: Comparison of SiC MOSFETs in 7pin D2Pak and 4pin TO-247 and their benefits for high-power MHz inverters," *IET Power Electron.*, vol. 12, no. 6, pp. 1349–1356, May 2019.

[139] T. Liu, T. T. Y. Wong, and Z. J. Shen, "A new characterization technique for extracting parasitic inductances of SiC power MOSFETs in discrete and module packages based on two-port S-parameters measurement," *IEEE Trans. Power Electron.*, vol. 33, no. 11, pp. 9819–9833, Nov. 2018.

[140] S. Li, L. M. Tolbert, F. Wang, and F. Z. Peng, "P-cell and N-cell based IGBT module: Layout design, parasitic extraction, and experimental verification," in *Proc. 27th Annu. IEEE Appl. Power Electron. Conf. Expo. (APEC)*, Mar. 2011, pp. 372–378.

[141] S. Li, L. M. Tolbert, F. Wang, and F. Z. Peng, "Stray inductance reduction of commutation loop in the P-cell and N-cell-based IGBT phase leg module," *IEEE Trans. Power Electron.*, vol. 29, no. 7, pp. 3616–3624, Jul. 2014.

[142] F. Yang, Z. J. Wang, Z. Zhang, S. Campbell, F. Wang, and M. Chinthavali, "Understanding middle-point inductance's effect on switching transients for multi-chip SiC package design with P-cell/N-cell concept," in *Proc. IEEE Appl. Power Electron. Conf. Expo. (APEC)*, Mar. 2018, pp. 1742–1749.

[143] M. Joko, A. Goto, M. Hasegawa, S. Miyahara, and H. Murakami, "Snubber circuit to suppress the voltage ringing for SiC device," in *Proc. PCIM Eur. Int. Exhib. Conf. Power Electron., Intell. Motion, Renew. Energy Energy Manage.*, May 2015, pp. 1–6.

[144] H. Zaman, X. Wu, X. Zheng, S. Khan, and H. Ali, "Suppression of switching crosstalk and voltage oscillations in a SiC MOSFET based half-bridge converter," *Energies*, vol. 11, no. 11, p. 3111, 2018.

IKER ARETXABALETA received the B.Sc. and M.Sc. degrees in telecommunications engineering from the University of the Basque Country, Bilbao, Spain, in 2014 and 2016, respectively, with a focus on electronics, and the Ph.D. degree in electronics from the University of the Basque Country, in 2021. Since 2016, he has been working as a Researcher with the Applied Electronic Research Team (APERT), Department of Electronic Technology, University of the Basque Country. His current research interest includes the application of power electronics in power converters.

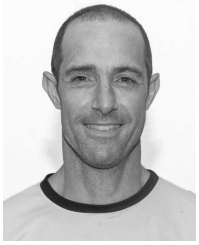

IÑIGO MARTÍNEZ DE ALEGRÍA received the B.Sc. and M.Sc. degrees in physics and the Ph.D. degree from the University of the Basque Country, Bilbao, Spain, in 1996 and 2012, respectively. For two years, he was with Ikerlan, a research center in mechatronics applications. Then, he was with Azterlan, a metallurgy research center. Since 2000, he has been an Associate Professor with the University of the Basque Country. His current research interest includes application of power electronics to renewable energies.

JON ANDREU received the M.S. degree in electronic and control engineering from the University of Mondragon, Mondragon, Spain, in 1997, and the Ph.D. degree in electronic and control engineering from the University of the Basque Country, Bilbao, in 2008. He was with Ideko Research Center, where he was involved in machine tools applications. Since 2002, he has been an Assistant Professor in electronic technology with the Department of Electronic Technology, University of the Basque Country, and became an Associate Professor, in 2011. His research interests include power converters and applications of power electronics.

IÑIGO KORTABARRIA received the M.Sc. degree in electronics and control engineering from the University of Mondragon, Spain, in 1999, and the Ph.D. degree in electronics and control engineering from the University of the Basque Country, Bilbao, Spain, in 2013. From 1999 to 2004, he was a research and development staff member in industrial electronics companies. From 2004 to 2014, he was an Assistant Professor in electronic technology with the Department of Electronic Technology, University of the Basque Country. In 2014, he became an associate professor. His current research interests include power converters and applications of power electronics.

ENDIKA ROBLES received the B.Sc. and M.Sc. degrees in telecommunications engineering from the University of the Basque Country, Bilbao, Spain, in 2015 and 2017, respectively, with a focus on electronics, where he is currently pursuing the Ph.D. degree in power electronics with the Electronic Technology Department. During these years, he was actively involved with the Applied Electronics Research Team (APERT), Engineering School of Bilbao. Likewise, during those years he worked closely with Tecnalia Research & Innovation Company, Derio, Spain, as an Educational Cooperation Student, with help from a college grant. Since 2017, he has been a Researcher in power electronics with the Electronic Technology Department, University of the Basque Country. His current research interests include the power conversion topologies and their modulation techniques.